Progress in Organic Coatings 192 (2024) 108529

Contents lists available at ScienceDirect

Progress in Organic Coatings

journal homepage: www.elsevier.com/locate/porgcoat

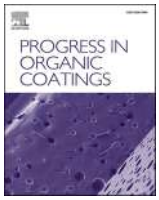

Enhancing wood coatings with red beetroot-derived pigments: Investigating synergy with UV absorber and composite filler for improved durability and aesthetics

Massimo Calovi *, Stefano Rossi

Department of Industrial Engineering, University of Trento, Via Sommarive 9, 38123 Trento, Italy.

ARTICLE INFO

Keywords:
Red beetroot
UV absorber
Composite filler
Wood paint
Coating durability

ABSTRACT

The objective of this study is to assess the synergy among a specific bio-based pigment derived from red beetroot, a composite filler, and a UV absorber as additives for wood paints. The composite filler aims to enhance the mechanical properties of the coating, while the UV absorber is selected to improve the pigment's color stability under solar radiation. The impact of these additives on sample aesthetics is evaluated through color, gloss, and roughness measurements. Mechanical properties are analyzed using Buchholz surface hardness and Taber abrasion resistance tests. The protective role of the UV absorber is further examined through accelerated degradation tests in a UV-B chamber. To ensure that the additives do not compromise the coating's barrier properties, water uptake tests, resistance to liquids, and contact angle measurements are conducted. Overall, the study demonstrates how each additive serves a distinct purpose and their combined application offers benefits such as enhanced color retention and improved mechanical durability of the coating. It highlights the potential of using bio-based pigments to enhance color durability without sacrificing the protective performance of wood coatings.

1. Introduction

The wood covering industry is experiencing continuous growth, attributed to the widespread use of wood materials. Wood presents numerous advantages, including its ease of manipulation [1], unique chemical [2], and physical [3] properties, and is widely availability. However, like many materials, it requires adequate protection through specific coatings. In this context, investigations into wood paints aim to improve their protective properties [4,5], seeking to address issues such as the degradation of their lignocellulosic components caused by factors such as sunlight exposure [6], moisture penetration [7], mechanical stress [8], chemical damage [9], and protection against harmful fungi [10].

Nevertheless, aesthetic is also pivotal in coatings, especially when it comes to wood. While wood has long been admired for its inherent natural beauty [11], there is now a growing emphasis on creating distinctive and visually striking finishes. For example, in the contemporary wood coatings industry there is a specific emphasis on achieving vibrant tones of color [12] by exploring and developing new functional pigments [13]. Simultaneously, similarly to many other industrial sectors, the wood industry is increasingly embracing the utilization of bio-based materials [14]. These innovative materials should be eco-friendly and align with the principles of the current circular economy. From this perspective, recent research has been dedicated to enhancing the coloring potential of alternative resources, such as microbes [15] and fungi [16,17]. Alternatively, other researchers have focused on developing colorants for wood coating sourced from wood by-products [18] dyes extracted from spices [19], and microalgae [20–22], achieving strong black, yellow and green tones, respectively.

Nevertheless, the adoption of bio-based materials often brings about significant challenges concerning the protective performance of the paint, its durability, and the color consistency of the *green* pigments themselves [14]. For instance, wood paints manufactured from bio-based materials frequently exhibit inadequate hardness and abrasion resistance [23], necessitating the addition of particular reinforcing fillers [24–27] to enhance these properties. Conversely, these bio-based pigments often reveal inadequate resistance to common phenomena such as photo-oxidation and decay when exposed to UV radiation [19,20]. Consequently, their incorporation as additives in paints for outdoor applications remains highly restricted [14].

* Corresponding author.
E-mail address: massimo.calovi@unitn.it (M. Calovi).

https://doi.org/10.1016/j.porgcoat.2024.108529
Received 1 March 2024; Received in revised form 29 April 2024; Accepted 15 May 2024
Available online 19 May 2024

Hence, the objective of this study is to develop and characterize a wood coating featuring pigments derived from bio-based materials, while also exhibiting excellent mechanical properties and consistent coloring even after exposure to outdoor conditions.

From this standpoint, red beetroot (*Beta vulgaris*) stands out as one of the most promising resources for extracting a pigment with potent coloring capabilities. Beetroot, belonging to the *Chenopodiaceae* family, thrives in temperate regions. It contributes significantly to global sugar production, accounting for approximately 20 % [28]. It is commonly consumed in various forms, including powdered, as a supplement juice, in bread, pickles, purees, boiled, and even processed into jam [29]. Furthermore, it is often used as an antibacterial [30] and antioxidant [31] additive, as it has high levels of betalains and other phytochemical compounds that are associated with antioxidant activity [32]. However, beetroot is highly valued above all for its strong coloring capabilities due to its abundant presence of water-soluble nitrogen pigments known as betalains [33], comprising betacyanins (red-violet pigments) and betaxanthins (yellow-orange pigments) [34,35]. As a result, recent studies have examined the utilization of red beetroot extracts in coatings [36], but have recommended their application solely for indoor use [37].

To enhance the effectiveness of pigments derived from red beetroot, it is feasible to utilize specific UV absorber materials. These substances act as light stabilizers by absorbing harmful UV radiation, thereby safeguarding the pigment from physical and chemical degradation, thus enhancing its color durability. Thus, this work, based on previous literature research, studies the effective role of *Uvasorb® S130*, a particular UV light absorber, in protecting the beetroot-based pigment. This type of additive has been extensively researched as a protective component in organic [38–40] and hybrid [41] coatings, often in conjunction with amine light stabilizers [42]. Moreover, its efficacy as a protective agent for wood coatings has been previously demonstrated [43].

Ultimately, it was determined that an innovative composite filler named *Polyfluo® 900* would be utilized to enhance the mechanical properties of the coating. This filler is composed of low-density polyethylene and PTFE, bolstered by ceramic microspheres. The selection of this specific additive is based on its tailored design aimed at enhancing abrasion resistance and surface durability, qualities notably absent in wood paints.

Hence, this study delves into the coloration properties of powder extracted from red beetroot, intended for use as a bio-based pigment in wood paints. The research explores its application alongside a designated reinforcing filler, aimed at enhancing the mechanical attributes of the coating. Additionally, to bolster the chromatic stability of the bio-based pigment under outdoor exposure, a UV absorber additive is incorporated into the coating formulation. Thus, this research underscores the potential for utilizing bio-based pigments in wood paints, with their mechanical attributes effectively enhanced through collaboration with composite fillers. This work is the first to show that beetroot waste can be utilized as a paint pigment, enabled by its interaction with a specific UV absorber. Additionally, the research investigates how an innovative composite filler can enhance the mechanical characteristics of wood varnish, an area that is frequently overlooked and underexplored. The study evaluates the durability of the coating and its protective capabilities through diverse accelerated degradation tests, while also assessing the consistency of aesthetic elements such as color and gloss in the composite layer.

2. Materials and methods

2.1. Materials

The beetroot powder was provided by Garzanti Specialties (Milan, Italy). The powder was acquired through the process of spray drying the fruit of *Beta Vulgaris*. It displays the characteristic purple-red hue and possesses an ash content of no more than 5.0 wt%. Subsequently, the product underwent manual grinding and sieving to achieve granules smaller than 40 μm. The composite filler *Polyfluo® 900* was supplied by Micro Powders (Tarrytown, NY, USA) and used as received. The substance is characterized as a composite material comprising low-density polyethylene (LDPE) and Polytetrafluoroethylene (PTFE), reinforced with ceramics, with the ceramic component consisting of microspheres based on alkali aluminosilicate. The powder exhibits white color and a melting point ranging from 121 to 132 °C, with a density of 1.02 g/cc and an average particle size falling within the range of 9 to 12 μm. *Uvasorb® S130* was provided by 3V Sigma (Bergamo, Italy) and used as received. It is a liquid UV absorber displaying a yellow to brownish hue, which comprises β-[3-(2-H-Benzotriazole-2-yl)-4-hydroxy-5-*tert*-butylphenyl]-propionic acid-poly(ethylene glycol) 300-ester + Bis[β-[3-(2-H-Benzotriazole-2-yl)-4-hydroxy-5-*tert*-butylphenyl]-propionic acid]-poly (ethylene glycol) 300-ester. It possesses a boiling point of 166 °C and a density of 1.17 g/cc. Poplar wood panels, measuring 150 × 150 × 2 mm^3, were procured from Cimadom Legnami (Lavis, TN, Italy). These panels exhibit a density within the range of 0.40 to 0.42 g/cm^3, and their moisture content falls between 6 % and 9 %. Chosen as the substrate for paint application, poplar plywood is renowned for its superior quality compared to other panel materials [44]. Its exceptionally smooth surface makes it well-suited for painting, laminating, or veneering [45]. Furthermore, its exceptional ease of machining, particularly its renowned reputation for effortless cutting, sanding, or screwing, positions it as the preferred option for crafting diverse samples intended for a wide array of characterization tests. The water-based acrylic paint, named *TECH20*, was provided by ICA Group (Civitanova Marche, AN, Italy). Formulated with materials obtained from sustainable and renewable sources, this paint product has a specific weight ranging from 1.01 to 1.18 g/ml and a viscosity of 50 to 60 s Ford Cup 5.

2.2. Samples production

In order to attain uniform paint coverage, the wooden base underwent a pre-treatment procedure involving the use of 320 grit paper to smooth the surface. Following this, the paint was applied using a spray method in accordance with the supplier's recommendations. The application process entailed utilizing a pressure of 3 bar and a material rate of 100 g/m^2. Four distinct sets of samples were produced, as detailed in Table 1, by modifying the paint composition through the addition of various additives. Sample REF sample was applied without any modification to the chemistry of the acrylic paint and served as a reference throughout the entire study. Its purpose was to facilitate a comparative assessment of the impact of the different additives incorporated into the formulation of the paint used for producing the other samples. Alternatively, sample B was created by incorporating 5 wt% of beetroot powder into the transparent waterborne paint. This amount of coloring powder was selected to achieve a vibrant color in the coating while avoiding any adverse effects such as pigment agglomeration, which could potentially disrupt the paint spraying process. In the paint utilized for producing sample BC, alongside the pigment, the composite filler was also incorporated. This was done with the aim of enhancing the mechanical properties of the paint, while simultaneously assessing its influence on the visual appearance of the coating. Lastly, the BCU

Table 1
Sample composition with relative nomenclature.

Samples nomenclature	Additives introduced in the paint formulation
REF	/
B	5 wt% beetroot powder
BC	5 wt% beetroot powder +5 wt% *Polyfluo® 900*
BCU	5 wt% beetroot powder +5 wt% *Polyfluo® 900* + 3 wt% *Uvasorb® S130*

sample was prepared using paint to which the UV absorber was additionally introduced. This was undertaken to mitigate the photodegradation phenomena commonly associated with natural organic pigments. The quantities of both *Polyfluo® 900* and *Uvasorb® S130* have been fine-tuned through initial investigations to ensure optimal performance without substantially altering the rheology of the paint or affecting its deposition process.

In order to ensure even dispersion of the different additives throughout the paint, each solution was mechanically mixed for 30 min prior to its application onto the wooden base. This mixing process ensured a homogeneous dispersion of the components in the solution, preventing sinking or floating phenomena. Subsequently, the painted coating was left to air cure for 4 h at room temperature.

2.3. Characterization

SEM observations were conducted employing the low vacuum scanning electron microscope SEM JEOL IT 300 (JEOL, Akishima, Tokyo, Japan) to analyze the morphology of both the bio-based pigment and the composite filler. Additionally, Energy-dispersive X-ray spectroscopy (EDXS, Bruker, Billerica, MA, USA) was used to assess their chemical compositions. Moreover, SEM was employed to examine the cross-sections of the coatings, elucidating the influence of the various additives on the structure of the composite layers. Optical stereomicroscope Nikon SMZ25 (Nikon Instruments Europe, Amstelveen, the Netherlands) was utilized to assess the aesthetics of the coatings, emphasizing the impact of the additives on the final coating's appearance. To achieve the same objective, colorimetric analyses were conducted using a Konica Minolta CM-2600d spectrophotometer (Konica Minolta, Tokyo, Japan) employing a D65/10° illuminant/observer configuration in SCI mode. Gloss measurements were performed using an Erichsen 503 instrument from Erichsen Co.Fo.Me.Gra Instruments (Co.Fo.Me.Gra, Milan, Italy), following the ASTM D523/14 standard [46]. 15 color and gloss assessments were conducted on 5 samples per series, with 3 measurements per sample.

The impact of the composite filler on the mechanical characteristics of the coatings was assessed through hardness and abrasion resistance tests. Coating hardness was examined using the Buchholz hardness indentation test, in accordance with the ISO 2815 standard [47]. An Elcometer 3095 Buchholz Hardness Tester (Elcometer, Manchester, UK) was employed, equipped with a beveled disc indentation tool featuring a sharp edge inserted into a stainless steel block. A consistent testing force of 500 g was applied for 30 s on the coating surface. The extent of the impression left by the standardized instrument served as an indicator of the coatings' hardness. 15 measurements were conducted on 5 samples per series, with 3 measurements per sample. The abrasion resistance of the coatings was investigated using the Taber test, conducted with a TABER 5135 Rotary Platform Abrasion Tester (Taber Industries, North Tonawanda, NY, USA), in accordance with the ASTM D4060–19 standard [48]. Two CS17 abrasion wheels were employed for this purpose. The samples underwent a total of 3000 Taber cycles, during which the extent of mass loss was monitored. Throughout the test, both color and gloss were observed to assess the evolution of the coatings' aesthetics. Following the experiment, the morphology and surface damage caused by the Taber grinding wheels were examined under SEM to analyze the behavior of the additives introduced into the paint. 3 samples per series were subjected to Taber testing.

To assess the aesthetic consistency of the coatings, the samples underwent accelerated degradation tests through exposure in a UV chamber for 48 h. A UV173 Box Co.Fo.Me.Gra (Co.Fo.Me.Gra, Milan, Italy) was utilized for this purpose, following the ASTM D4587-11 standard [49]. This procedure entails exposure to UV-B radiation (313 nm) at 60 °C. The standard mandates the use of intense UV-B radiation, which only partially replicates the samples' exposure to solar radiation. However, this particular test was chosen specifically to highlight the potential reinforcing effect of the UV absorber, which can reduce the color change observed in the beetroot-based pigment when exposed to intense radiation. Colorimetric and gloss analyses were conducted during the exposure period to assess the aesthetic consistency of the coatings and investigate the influence of specific additives. Furthermore, the FTIR spectra of both the pigment and the composite filler were obtained in attenuated total reflection (ATR) mode using a Varian 4100 FTIR Excalibur spectrometer (Varian Inc., Santa Clara, CA, USA), both before and after the UV-B exposure test. These measurements were conducted to assess any chemical modifications occurring in the additives as a result of UV exposure. The exposure was halted after 48 h due to significant degradation observed in the samples, with noticeable differences depending on whether the UV absorber was present or absent.

The various additives were incorporated to impart specific color to the coating and enhance its mechanical strength and resistance to ultraviolet radiation. However, to ensure that these additives do not compromise the barrier properties of the coating, the samples underwent various tests. The liquid water absorption test was conducted according to the EN 927-5:2007 standard [50] to evaluate the water permeability of the coatings. 5 uncoated surfaces of the 40 × 40 × 2 mm^3 poplar wood panels were sealed hermetically with silicone to prevent water absorption by the wood substrate. The samples were preconditioned at 65 % relative humidity and 20 °C before being immersed in a container filled with water. The moisture absorption, expressed in grams per square meter (g/m^2), was determined by measuring the change in mass before and after 6, 24, 48, 72, and 96 h. 5 samples per series were subjected to the analysis. The cold liquid resistance test was employed to evaluate the coatings' resistance to various chemical substances, following the UNI EN 12720 standard [51]. In this experiment, filter paper was immersed in separate solutions containing 15 % sodium chloride, pure acetone, olive oil, and coffee. Furthermore, the resistance of the coatings to acidic and basic conditions was assessed using solutions with pH levels of 1 and 14, respectively, achieved by employing concentrated HCl and NaOH. These soaked filter papers were then placed onto the surface of the coating and covered with a glass lid. Following the 24-h period, the glass cover and filter paper were removed, and any residual liquid on the coating surface was carefully eliminated. Both the liquid water absorption test and the cold liquid resistance test were associated with color and gloss measurements, to evaluate the aesthetic consistency of the coatings.

Lastly, contact angle measurements were conducted following the ASTM D7334–08 standard [52] to assess the influence of different additives on the coating's wettability. Macro images were captured using a Nikon 60 mm lens with an aperture of f/2.8 (Nikon Instruments Europe, Amstelveen, the Netherlands). The contact angle measurement was performed using the NIS-Elements Microscope Imaging software (Windows Version 4.30.01). Demineralized water droplets (5 μl), were generated via a syringe and dispersed from approximately 2 cm away. After 60 s of being placed on the coating, the droplet was photographed, and the wetting angle was determined using the imaging software. The wait of the 60 s was taken precisely to highlight the solidity of the behavior of the samples, and to monitor possible evolutions in the behavior of the coatings. To ensure statistical reliability, each sample was subjected to 10 measurements, allowing for a thorough examination of the surface wettability characteristics. The contact angle measurements were coupled with surface roughness analyses of the coatings, conducted using the MarSurf PS1 mobile surface roughness measurement instrument from Carl Mahr Holding (Gottingen, Germany). This additional analysis aimed to provide insight into the wettability outcomes observed across the different samples.

3. Results and discussion

3.1. Fillers and coatings appearance

The UV absorber *Uvasorb® S130* is a liquid with a yellow to brownish

color, whereas the other two additives studied are solid micro-powders, which can be analyzed using SEM observations. Fig. 1 depicts the morphological characteristics of the two active substances, observed using SEM in secondary electrons mode. The beetroot powder (Fig. 1a) exhibits a jagged surface morphology and variable sizes. Nevertheless, due to the sieving process, the granules have a size of less than 40 μm, frequently ranging in the order of tens of micrometers. They possess a homogeneous composition primarily consisting of organic materials. EDXS analysis has revealed a significant presence of carbon, oxygen, and potassium, along with traces of sodium, magnesium, silicon, and chlorine. The analysis result is illustrated in **Fig. S1** in the Supplementary Materials. In contrast, the composite filler (Fig. 1b) is composed of two distinct materials: granules of varying sizes and irregular morphology, and more uniform microspheres. The granules constitute the organic component of the filler, while the spheres are composed of ceramic material. **Fig. S2** in the Supplementary Materials displays the elemental analysis of the spheres, confirming their alkali aluminosilicate composition. The granules exhibit variable dimensions, averaging around 10 μm, as confirmed by the manufacturer, while the microspheres are generally smaller, with diameters typically less than 10 μm. Both types of additives, namely beetroot powder and composite filler, possess relatively small dimensions, making them well-suited for incorporation into organic coatings.

Hence, the three additives (including also the UV absorber) were utilized in various formulations of the acrylic paint, resulting in the creation of four series of samples as detailed in Table 1. Fig. 2 showcases the appearance of these samples, observed both from a top-view and in cross-section using an optical microscope. This observation underscores how the aesthetics of the coatings are significantly influenced by the incorporation of different additives into the paint. The transparent paint applied to sample REF (Fig. 2a) accentuates the natural aspect of the poplar wood substrate. Conversely, the incorporation of beetroot pigment results in a vibrant red hue for the coating of sample B (Fig. 2b). The red color gradually transitions in shade within sample BC and sample BCU (Fig. 2c and Fig. 2d, respectively), shifting towards hues leaning more to orange. This shift is attributed to the inclusion of the composite filler in sample BC, whose white color contrasts with the red pigment, and the yellow component of the wooden substrate. This effect is further pronounced in sample BCU, which also contains the yellow UV absorber. Indeed, the incorporation of additives not only leads to aesthetic alterations but also induces morphological changes in the coating. The images indeed provide insight into the internal structure of the coatings, as observed under SEM. The micrographs emphasize how the addition of the pigment introduces a degree of structural complexity, further accentuated by the presence of the composite filler, as evidenced by the presence of the ceramic microspheres. The inclusion of additives, however, does not result in the formation of notable defects, such as porosity or voids at the interface with the fillers. Additionally, it does not affect the coating deposition process, as the layers of the four samples exhibit comparable thickness, approximately 160 μm.

Thus, the most significant alteration brought about by the additives primarily pertains to the aesthetic attributes of the coatings, as qualitatively depicted by the images in Fig. 2. However, a more detailed and quantitative description of these changes is provided by the graphs presented in Fig. 3. Fig. 3a illustrates the gloss values of the coatings, which vary depending on the additive incorporated into the paint formulation. Sample REF demonstrates high reflectance, with gloss values around 50. The introduction of the pigment in sample B results in a notable reduction in reflectance, rendering the coating slightly more opaque. However, the inclusion of the composite filler causes a significant decrease in gloss values, making sample BC particularly opaque. This effect is somewhat mitigated with the additional incorporation of the UV absorber into sample BCU, although it still retains a considerable level of opacity. These phenomena can be attributed to varying roughness values across the four series of coatings, as depicted in Fig. 3b. The graph presents both the roughness values measured longitudinal (Ra//) to the fibers of the wooden support and those assessed perpendicular (Ra⊥) to them. Considering that the coating adheres closely to the morphology of the wooden substrate, it is typical to anticipate higher roughness in the direction perpendicular to the fibers. Indeed, the Ra values are consistently higher in the direction perpendicular to the fibers compared to those measured lngngitudinal to the fibers, and they are comparable across all four sets of samples. The primary variation lies in the level of lngngitudinal roughness, Ra//. Sample REF displays relatively low Ra// values, contributing to its reflective nature. Similarly, sample B also exhibits low Ra// values, indicating that the reduction in reflectance is primarily attributed to the presence and aspect of the pigment itself. In contrast, the incorporation of the reinforcing filler in sample BC and sample BCU results in a significant rise in roughness, leading to a noticeable enhancement in surface opacity. This observation corroborates the earlier hypotheses regarding the morphological alterations introduced by the filler in the coating, which consequently yields significant aesthetic implications by modifying the surface texture and reflectance of the composite layer. Moreover, the additional incorporation of the UV absorber in sample BCU results in a slight decrease in roughness values, accompanied by an increase in gloss. This additive, being in liquid form, serves as a levelling agent, mitigating the rise in roughness induced by the composite filler, albeit to a limited degree.

Indeed, as emphasized by the optical images in Fig. 2, it is primarily the color of the coatings that undergoes significant alterations upon the introduction of various additives into the transparent paint. Fig. 3c displays the color change values (ΔE), measured relative to the reference sample REF. ΔE has been calculated employing the following relationship [53]:

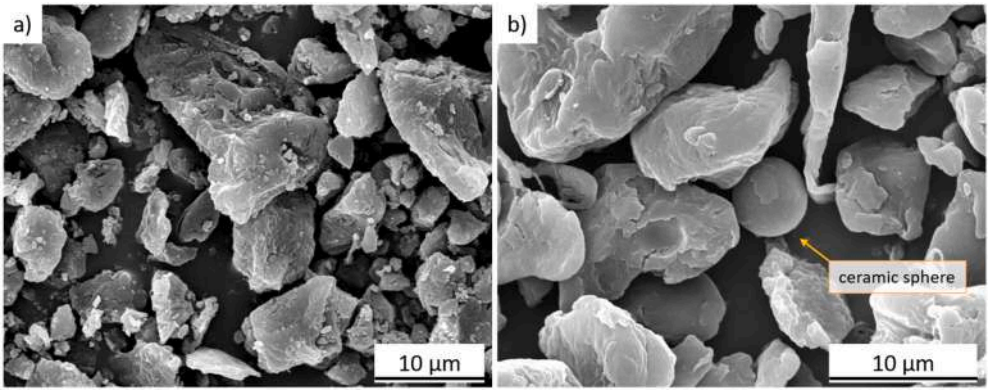

Fig. 1. SEM images depicting a) the red beetroot pigment and b) the composite reinforcing filler, acquired in secondary electrons mode. (For interpretation of the references to color in this figure legend, the reader is referred to the web version of this article.)

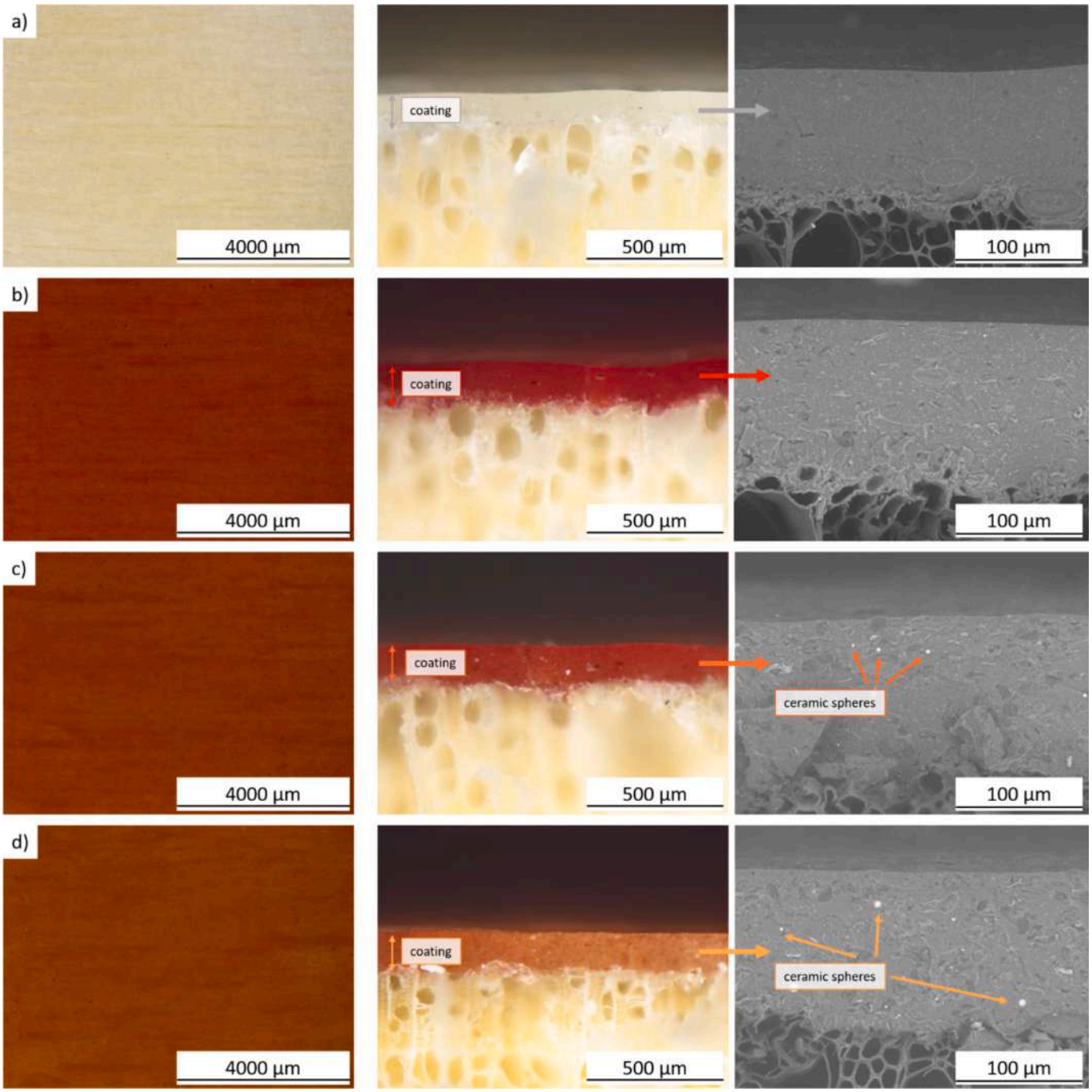

Fig. 2. Optical micrographs showcase of the top-view (on the left) and cross-section (on the right) of a) sample REF, b) sample B, c) sample BC, and d) sample BCU. Additionally, a SEM-acquired enlargement of the cross-section of the coatings is featured on the right.

$$\Delta E = \left[(\Delta L^*)^2 + (\Delta a^*)^2 + (\Delta b^*)^2 \right]^{1/2} \quad (1)$$

In colorimetry, the coordinates L*, a*, and b* denote specific attributes of color:

- L* represents lightness, with a scale from 0 (for black objects) to 100 (for white objects);
- the a* axis represents the red-green axis, where positive values indicate redness and negative values indicate greenness;
- the b* axis represents the yellow-blue axis, where positive values indicate yellowness and negative values indicate blueness.

The three series of composite coatings demonstrate significant color change values (ΔE), ranging between 42 and 45 points compared to sample REF. These values are considerable, particularly given that some studies suggest the human eye can discern and appreciate color changes of only one unit [54]. Hence, it can be concluded that the beetroot-derived powder possesses an exceptionally potent coloring capability, as evident in Fig. 2 as well. It's intriguing how, despite the distinct appearances of the three composite coatings due to varying additive contents, they exhibit color changes comparable to the REF sample. This phenomenon is elucidated by the graph in Fig. 3d, which illustrates the values of the individual CIE Lab coordinates for the four series of samples. The lightness values (L*) of the three composite coatings are similar, yet notably lower than that of sample REF. The introduction of

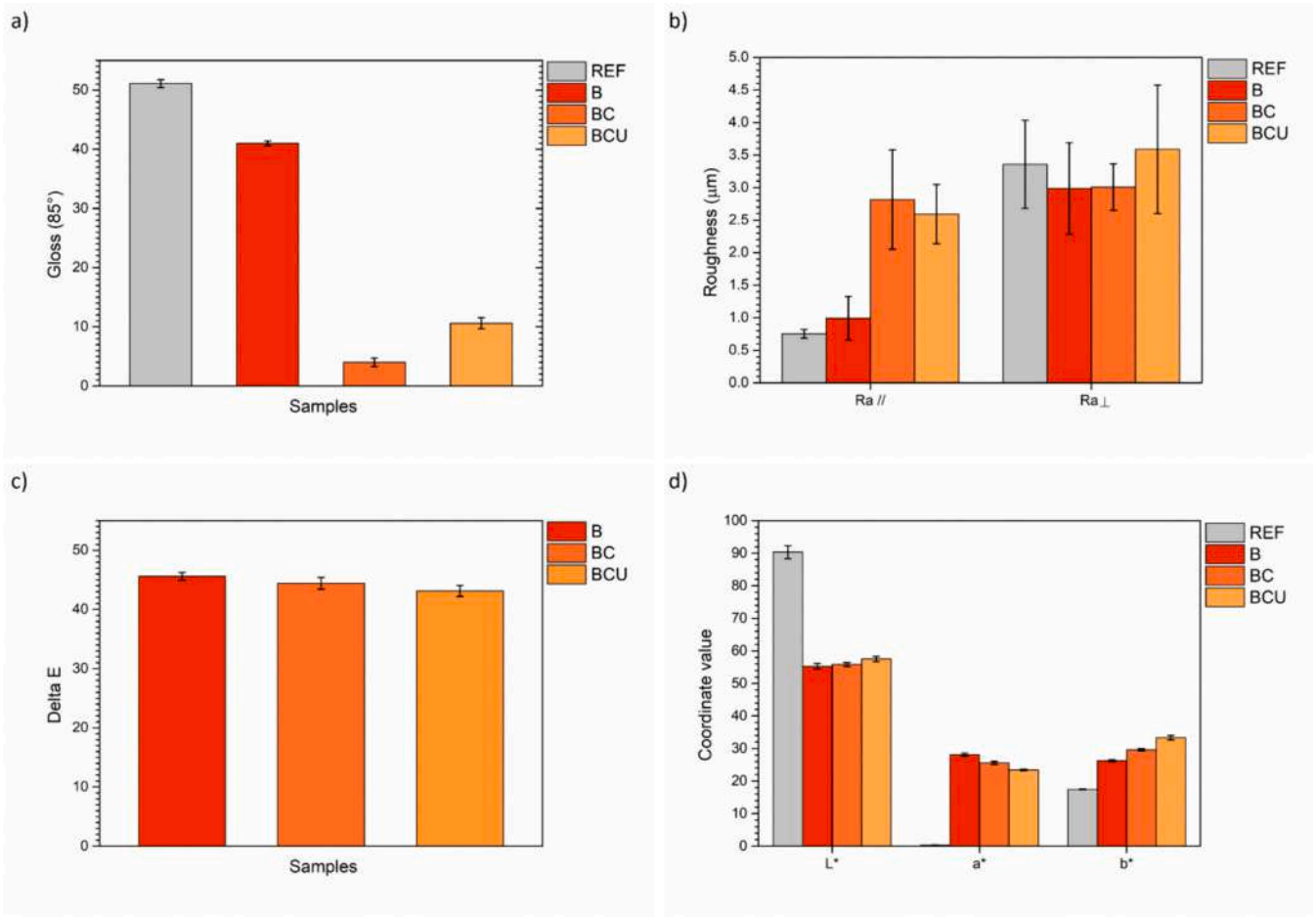

Fig. 3. a) Disparity in gloss among the four series of samples, b) coatings surface logngitudinal (Ra//) and perpendicular (Ra⊥) roughness, c) changes in color relative to the reference sample REF and d) corresponding values of the three CIE Lab coordinates L*, a* and b*.

the pigment results in a significant increase in the a* coordinate, shifting towards red hues, and in the b* coordinate, trending towards yellow tones. However, the addition of the composite filler (BC) followed by the UV absorber (BCU) gradually decreases the a* coordinate while increasing the b* coordinate. Consequently, although the individual color coordinates of the samples vary, the formula (1) used for calculating ΔE yields very similar results for the three composite samples, as the decrease in a* corresponds to the increase in b*. Indeed, each individual additive exerts a distinct influence on the aesthetics of the coating, resulting in a unique color for each sample series. Undoubtedly, the beetroot pigment plays the most significant role, yet the contribution of the composite fillers and the UV absorber should not be underestimated. Each additive contributes to the overall appearance and color of the coating, highlighting the complexity of their combined effects on the final product.

In conclusion, all three additives are viable for use in wood coatings, as they do not introduce significant defects or disrupt the paint spraying process. However, the beetroot-derived pigment imparts intense coloration, while the composite reinforcing filler alters the coating's texture by increasing its roughness and decreasing the overall reflectance. Moreover, the unique synergy among the additives produces a distinct color in the coating, emphasizing the importance of dosing each material according to the desired aesthetic outcome in the final product.

3.2. *Impact of the additive on the coating's mechanical characteristics*

Given the typically low mechanical properties of clearcoat paints [55,56], this study aimed to assess the impact of a novel composite reinforcing filler added to sample BC and sample BCU. The primary focus was on addressing concerns regarding the hardness and subsequent abrasion resistance of the coating, with a specific emphasis on examining the contribution of this particular additive.

Fig. 4a illustrates the results of the Buchholz hardness test, displaying the average length of indentations formed in the coatings alongside the Buchholz hardness value. It is readily apparent that the presence of the composite filler enhances the mechanical properties of the coating, as evidenced by a decrease in the length of the indentation correlating with an increase in the hardness of the layer. While sample REF and sample B demonstrate identical behavior, indicating a negligible impact of the beetroot pigment on coating hardness, sample BC and sample BCU exhibit notably reduced average indentation lengths. The addition of 5 wt% filler leads to an improvement of approximately 10 % in terms of reducing the length of the indentation in the coating. Similar results have been observed in previous studies utilizing bio-based fillers, such as cellulose microfibers [23] and polyamide 11 powders [24]. However, one of these studies highlighted a notable challenge associated with the easy agglomeration of the microfibers, resulting in reduced coating performance [23]. Conversely, achieving the same outcome demonstrated by the *Polyfluo® 900* composite filler required a larger quantity of polyamide 11-based additive [24]. Another study demonstrated the potential for achieving improved results through the utilization of functional fillers, such as stainless steel flakes. However, it was observed that even in this scenario, the required quantity of additive significantly surpassed that utilized in the present study [57].

Despite the observed increase in hardness, it cannot be considered significant as it remains below the value of 50 on the Buchholz scale.

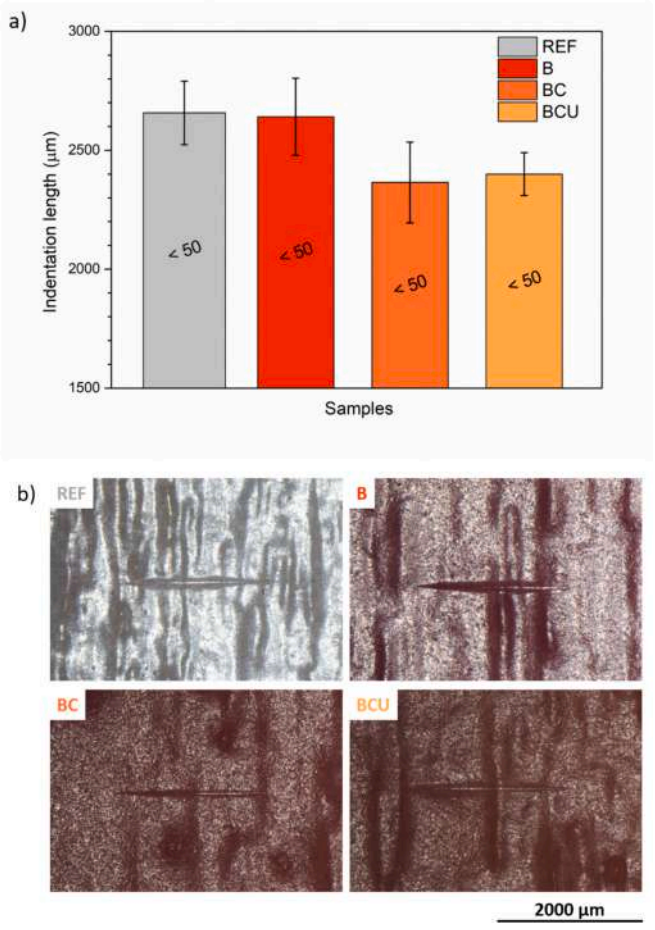

Fig. 4. a) Mean indentation imprint sizes observed in Buchholz hardness testing, along with their corresponding Buchholz hardness readings. b) Optical microscope images depicting Buchholz test notches.

Essentially, while the composite fillers indeed exhibit higher hardness compared to the pure acrylic matrix of the coating, they do not distinctly enhance the system at the current concentrations investigated in this study. In fact, the images obtained with the stereo microscope in Fig. 4b, illustrating examples of imprints caused by the Buchholz indenter, show minimal differences between the four series of samples.

Thus, it can be concluded that the acrylic matrix of wood paint is inherently soft, making it challenging to significantly enhance its hardness through the addition of solid fillers. Achieving a substantial reinforcing contribution would likely necessitate high quantities of additives, which could unavoidably alter the structural morphology of the coating and potentially affect other of its properties, such as the layer's barrier performance.

On the contrary, the composite filler seems to make a notable contribution in terms of the abrasion resistance of the coating, as emphasized by the graph in Fig. 5. The graph illustrates the trend of the mass lost during the Taber abrasion test, where the wheels exert high abrasive forces on the surface of the composite layers. Since the density of the three additives and the paint is comparable, a reduced mass loss of the coatings can be associated with an improvement in their abrasion resistance. Sample B demonstrates a trend very similar to that of sample REF, but also a slight increase in mass lost during the initial Taber cycles. This outcome suggests that the addition of the pigment causes a minimal reduction in the surface resistance features of the coating, possibly due to a decrease in the compactness of the polymer binder, whose chains are interrupted by the presence of the coloring powder. Conversely, sample BC and sample BCU exhibit practically overlapping trends and

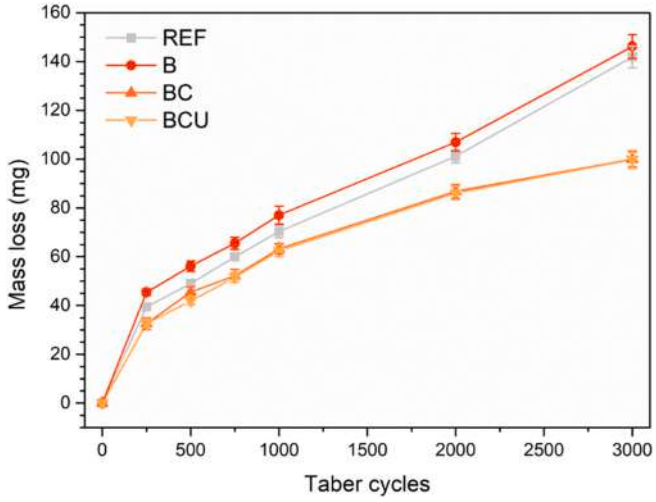

Fig. 5. Variation in coating mass loss relative to the number of Taber cycles.

results, which are superior to those of the two previous samples. Their mass loss remains consistently lower than that of the REF and B samples, with this disparity increasing during the test. This underscores an enhancement in the abrasion resistance characteristics, attributed to the substantial contribution of the composite filler, which is present in larger quantities within the bulk of the coating rather than directly on the surface of the layer. Moreover, the identical behavior observed in both sample BC and BCU demonstrates that the additional presence of the UV absorber in the latter does not affect the protective attributes provided by the composite filler. At the conclusion of the test, following 3000 Taber cycles, sample BC and sample BCU demonstrate a reduction in mass loss equivalent to 29 % compared to sample REF. Comparable outcomes in wood paints were attained through the addition of polyamide 11 [24] or magnetite powder [57], albeit in larger quantities. Conversely, certain types of fillers, such as cellulose nanocrystals [9,58], failed to achieve similar performances due to agglomeration phenomena, inevitably resulting in reductions in the abrasion resistance of the coating.

In order to elucidate the protective mechanism of the composite filler more precisely, SEM analysis was conducted on two samples, namely REF and BC, to examine their surface morphology before and after exposure to the abrasive stresses of the Taber test. Fig. 6a illustrates the top-view appearance of sample REF. Initially (left), the coating appears notably flat and devoid of defects. However, following the Taber test (right), the surface displays pronounced damage characteristic of the abrasive action of Taber grinding wheels [24,59,60]. In contrast, the appearance of sample BC (Fig. 6b) exhibits distinct differences both before and after the abrasion resistance test. Initially, the sample reveals numerous indications of the composite filler on the surface, represented by the lighter areas. Since the images were captured in secondary electrons mode, these lighter traces indicate a complex surface morphology, which is not flat but rather enriched with asperities, precisely represented by the filler. By comparing this image with the corresponding REF sample, it becomes evident the actual enhancement in surface roughness induced by the composite filler, as previously illustrated in Fig. 3b. It's intriguing to note a distinctive surface morphology of sample BC following the abrasion test: unlike sample REF, the same abrasion traces are limited, replaced by a noticeable reinforcing effect exerted by the composite filler. Specifically, the organic component of the filler tends to undergo a "smearing" effect due to the cutting forces from the abrasive wheels. This process results in the formation of a highly lubricious surface, akin to phenomena previously documented in the literature with wax-based additives [19,22]. This highly lubricious surface significantly mitigates abrasion processes and consequent material removal, providing a rationale for the superior performance

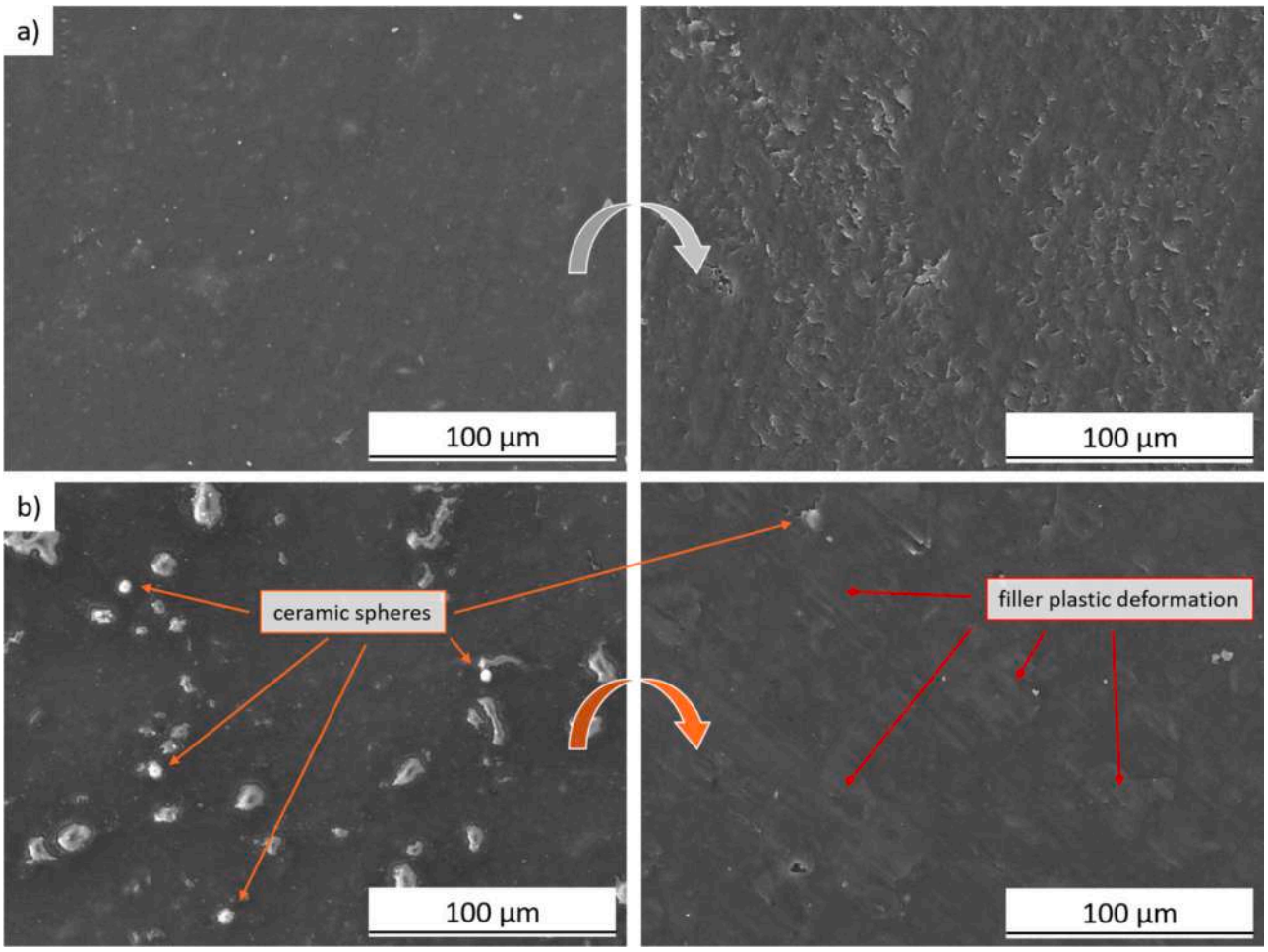

Fig. 6. SEM micrographs of the surface morphology of a) sample REF and b) sample BC, before and after the Taber test (left and right, respectively).

observed in sample BC and sample BCU as depicted in Fig. 5. It is evident that this self-lubricating phenomenon on the surface is attributed to the presence of the PTFE component within the composite filler. PTFE is widely recognized for its exceptionally low coefficient of friction [61,62], which facilitates the creation of a slippery surface, thus contributing to the observed self-lubrication effect [63]. Consequently, although the hard ceramic microspheres do not notably enhance the coating's hardness, the presence of the PTFE component significantly improves the wood coating's resistance to abrasion.

Therefore, PTFE exhibits superior reinforcing performance compared to other environmentally-friendly additives like polyamide 11, cellulose fibers, and magnetite powders. However, its use is not without drawbacks, particularly concerning environmental aspects [64]. Perfluorooctanoic acid (PFOA), commonly used in PTFE synthesis, poses toxicity concerns due to its persistence in the environment and long human half-life, leading to potential toxicity upon continuous accumulation [65]. In response, PFOA is being replaced by chemicals like perfluoro-2-propoxypropanoic acid (PFPrOPrA, Trade name: GenX), which, although potentially toxic, are less bio accumulative [66]. Short-chain alternatives are also recommended for their rapid clearance from the human body, despite lingering questions about their environmental persistence and health effects [67].

To address toxicity and sustainability concerns, many companies are exploring alternative products that do not contain PTFE but still offer effective functional properties [68]. Nonetheless, this study underscores that PTFE-based additives remain unmatched in enhancing the abrasion resistance of organic coatings, with previously discussed waxes presenting the only true "*green*" alternative to this type of additive.

Fig. 7a displays the current appearance of the samples at the end of the test, showcasing the characteristic circular imprints caused by the Taber grinding wheels. These imprints are also distinctly visible to the naked eye, as the abrasive process induces a modification of the surface texture. To assess the chromatic and aesthetic consistency of the coatings, the color change and gloss values were monitored throughout the abrasive test. Fig. 7b illustrates the evolution of the color of the samples during the test, revealing a chaotic trend of limited and almost negligible extent. In contrast, Fig. 7c demonstrates how the abrasion process significantly modifies the gloss values of the four series of samples during the initial cycles, eventually reaching a plateau value. This phenomenon arises from an initial alteration in the surface roughness of the samples, which then remains constant throughout the abrasive test. While the degree of reflectance of sample REF and sample B decreases due to a slight increase in roughness, the abrasive processes tend to diminish the initially high roughness values of sample BC and sample BCU, resulting in an increase in gloss. Consequently, the abrasive mark is clearly discernible due to substantial changes in gloss, either reduced (REF and B) or increased (BC and BCU).

In conclusion, the composite filler does not substantially enhance the surface hardness of the coating, likely due to the limited quantity of hard ceramic microspheres. Nevertheless, PTFE component imparts a self-lubricating effect on the surface, enhancing resistance against material removal during abrasive processes. While these abrasive effects unavoidably alter the aesthetics of the samples by modifying their reflectance values, they do not affect the color imparted by the bio-based pigment.

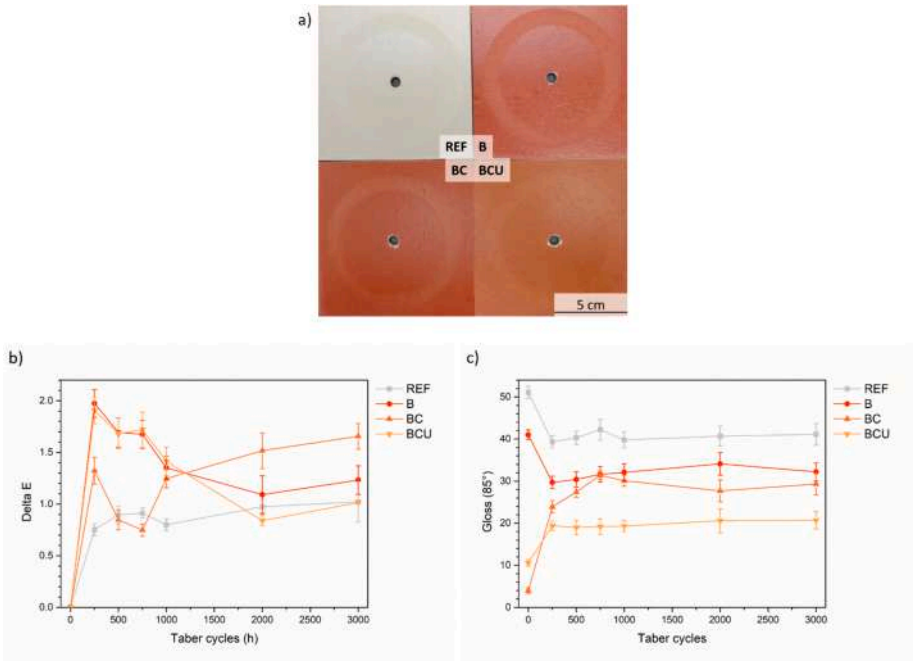

Fig. 7. a) images capturing the surface condition of the samples upon completion of the test and evolution of b) color and c) gloss of the samples throughout the duration of the Taber test.

3.3. Influence of the additive on the coating's ability to withstand solar radiation

A frequent issue observed with the utilization of natural and bio-derived pigments is their inherent inclination towards physical and chemical deterioration upon exposure to sunlight [69]. Additionally, red dyes and pigments tend to be less stable compared to others [70], owing to factors associated with the chemical composition of the pigments utilized and the characteristics of the light they absorb. Given that red occupies the lower energy range of the visible light spectrum, the pigment must absorb all higher energy wavelengths to appear as red. It is this absorption of high-energy photons that leads to the breakdown of the pigment and diminishes its intensity of "redness" [71].

Hence, a UV absorber was incorporated into sample BCU to enhance

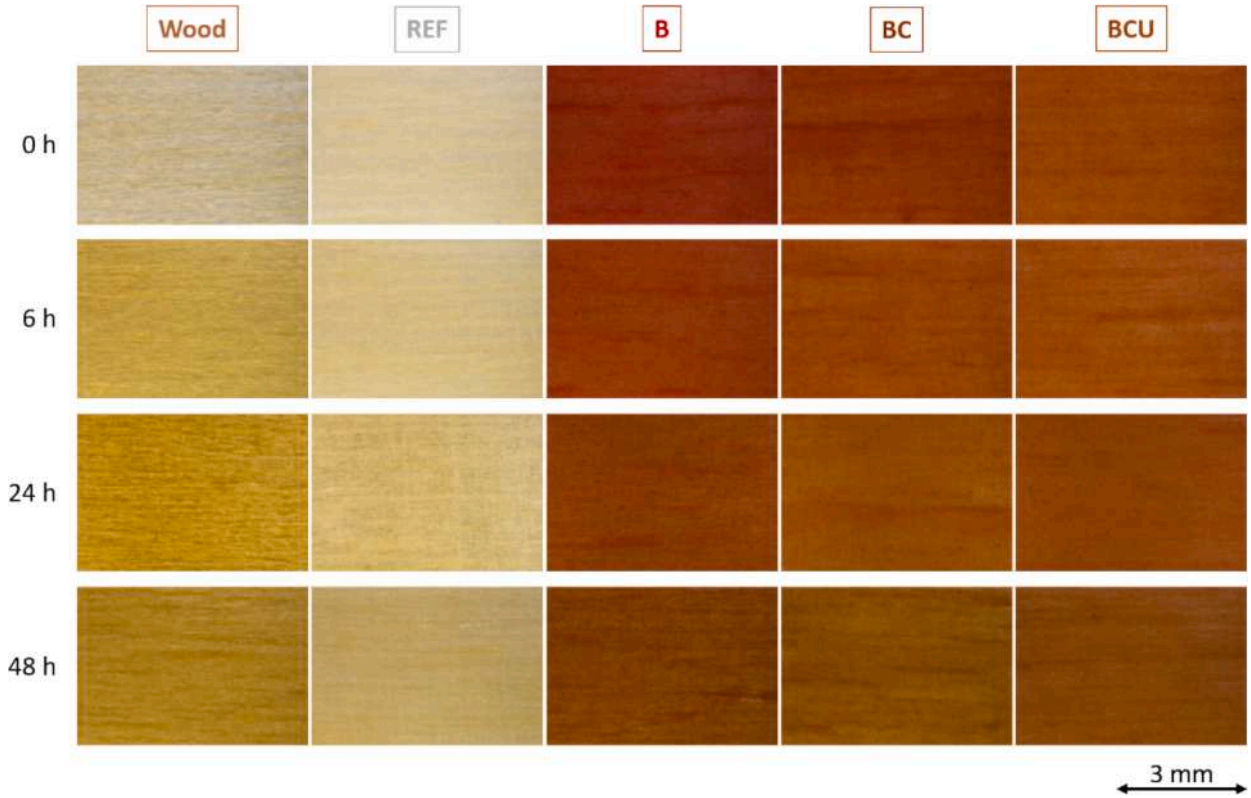

Fig. 8. Alteration of the appearance of both the wooden panel and the coated samples due to exposure to UV-B radiation.

the pigment's longevity and thereby maintain the aesthetic uniformity of the coating over time. To assess the effectiveness of this protective additive, the samples underwent exposure in a UV-B chamber, undergoing rigorous accelerated degradation tests. Fig. 8 illustrates the progression of the samples' appearance, including the individual wooden substrate, throughout the duration of the test. A significant deterioration of the wooden sample, characteristic of this material, is clearly noticeable, resulting in yellowing and darkening of the poplar panel. Sample REF also exhibits a slight darkening, which is not associated with photodecay processes of the acrylic paint, known for its resilience to UV radiation. Previous studies have indicated that the transparent coating does not entirely block UV radiation, resulting in a minor degradation of the wooden substrate, which becomes visible due to the coating's transparency [72]. As anticipated, sample B appears to be notably affected by UV-B radiation exposure, undergoing a considerable color transformation from initial red tones to a dark brown hue, indicative of the degradation of the beetroot pigment. Likewise, albeit to a lesser extent in lighter shades, sample BC shows noticeable degradation. Conversely, the process of aesthetic decay appears to be restrained in sample BCU.

The degradation observed in sample B and sample BC is likely attributed to the low resistance of the bio-based pigment, as supported by the images in Fig. 9. These images, acquired with the stereomicroscope, depict the progression of the appearance of the pigment and the composite reinforcing filler when individually exposed to a UV-B chamber for 48 h. The pigment extracted from beetroot (Fig. 9a) initially displays a vivid color, featuring purple-burgundy tones characteristic of its vegetable origin. However, after the accelerated degradation test, the powder undergoes a striking chromatic shift, losing its distinct hue and acquiring yellow shades. This alteration is attributed to typical photooxidation phenomena affecting the betacyanins abundant in the pigment [73]. In fact, betacyanins are susceptible to degradation induced by various factors, including temperature [74], pH [75], and most significantly, exposure to light [34]. Studies have shown that betacyanins have the ability to absorb visible light, and differences in their chemical structures influence their light-absorbing properties [76,77]. Moreover, betacyanins are unstable and prone to degradation in the presence of oxygen and light at elevated temperatures. Light exposure can promote the degradation of betacyanins, particularly within the ultraviolet to visible light spectrum, triggering transitions from electron-excited states to more reactive chromophore states [78]. Furthermore, the degradation of betacyanins under light conditions is oxygen-dependent; the effects of light exposure are minimal under anaerobic conditions [79]. Therefore, the combination of UV-B radiation, oxygen, and exposure to 60 °C temperature during the test accelerates the rapid and inevitable degradation of the red beetroot-based pigment.

Conversely, the composite filler (Fig. 9b) does not seem notably impacted by UV-B radiation exposure. Actually, despite being made of low density polyethylene, which is prone to photooxidative degradation [80], the filler also includes substances that have strong UV-B radiation resistance, such as PTFE [81] and aluminosilicate alkalis.

Thus, the two active ingredients underwent FTIR analysis before and after the exposure to the accelerated test to examine any chemical changes induced by UV-B radiation. In Fig. 10, the spectra of the two additives are depicted before and after 48 h of exposure in the UV chamber. The pigment derived from beetroot exhibits a characteristic band at 3226 cm^{-1}, indicative of the stretching vibration of the –OH bond attributed to hydroxyl groups [82]. Additionally, the peak at 2941 cm^{-1} is associated with the vibrational stretching of the C—H bond due to alkanes [83]. The presence of betalains, typical N-containing compounds of beetroot, is indicated by the peak at 1614 cm^{-1}, corresponding to the stretching vibration of the C═N bond [84]. Furthermore, the signal at 1345 cm^{-1} corresponds to the C—H aliphatic bending of organic compounds, the band at 1236 cm^{-1} represents to the stretching vibration of the C—O bond of the carboxylic acid [83,85], while the peak at 1067 cm^{-1} represents the symmetric stretching vibration of the C–O–C link [86]. Moreover, the signal at 989 cm^{-1} corresponds to the bond deformation of the C—H bond and the aromatic C—H in-plane bending [87], whereas the peak at 909 cm^{-1} can be

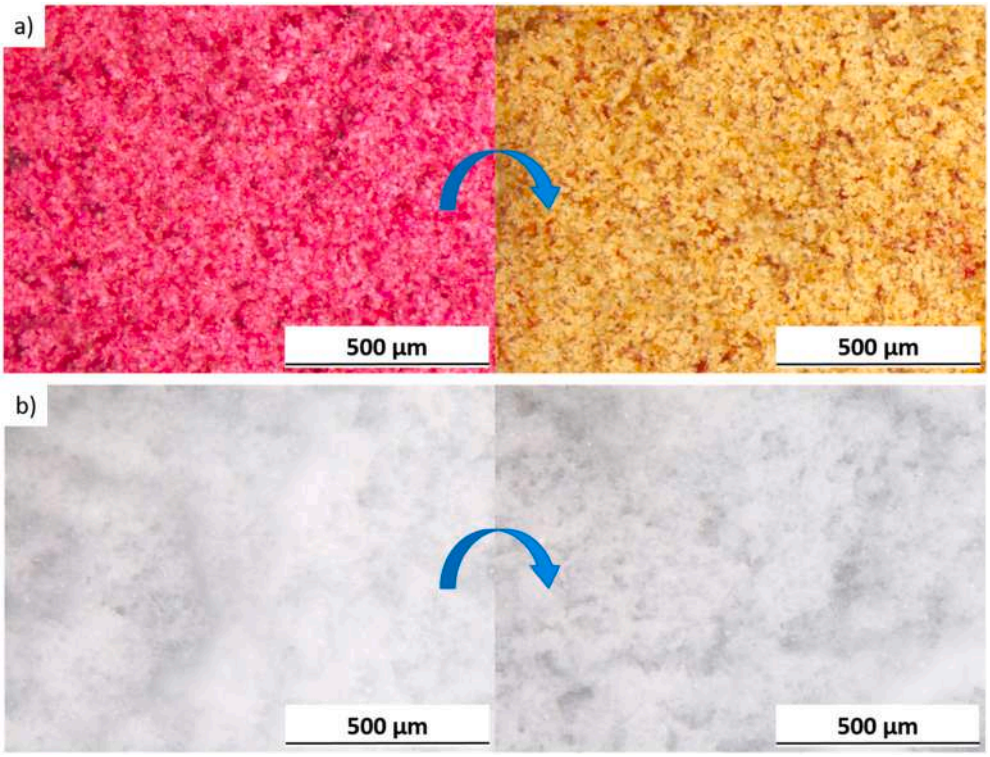

Fig. 9. Optical images illustrating the alteration in appearance of a) the bio-based pigment and b) the composite filler after being subjected to UV-B radiation for 48 h.

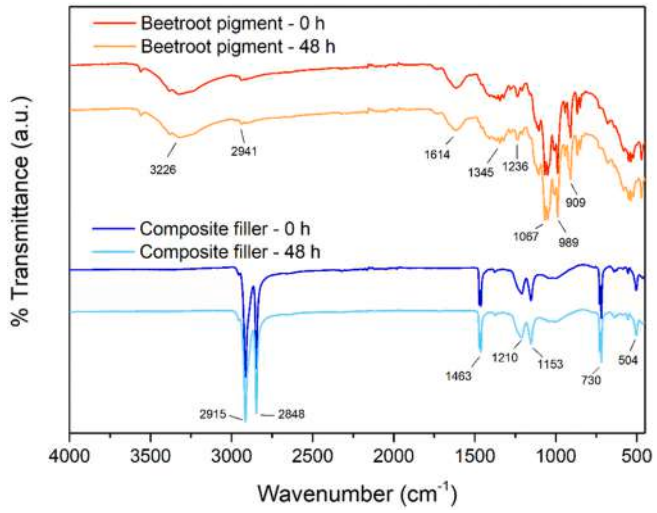

Fig. 10. FTIR spectra of the pigment and composite filler before and after 48 h exposure to UV-B radiation.

associated with the stretching vibrations of the C–COOH bond for carboxylic acids [88].

In contrast, the spectrum of the composite filler reveals two prominent peaks at 2915 cm^{-1} and 2848 cm^{-1}, indicative of CH_2 asymmetric and symmetric stretching, respectively. Additionally, the signal at 1463 cm^{-1} can be attributed to bending deformations, while the signal at 730 cm^{-1} corresponds to rocking deformation. These signals signify the presence of LDPE in the compound [89]. Furthermore, the presence of PTFE is indicated by the characteristic peaks at 1210 cm^{-1} and 1153 cm^{-1}, associated with asymmetric and symmetric CF_2 stretching, respectively [90]. Furthermore, a third peak at 504 cm^{-1} can be attributed to CF_2 wagging [91]. Lastly, the presence of aluminosilicate spheres, albeit in smaller quantities compared to the organic component of the filler, is indicated by a subtle band at 1000 cm^{-1}, attributed to the vibration of the SiO/Al–O bond within the aluminosilicate framework [92,93].

Despite the evident aesthetic changes observed in the pigment due to photooxidation processes, FTIR analysis fails to discern this phenomenon, as the two spectra of the material derived from beetroot are nearly identical. Similarly, the composite filler, despite not exhibiting obvious changes in appearance, also shows no discernible differences in FTIR spectra. However, it is noteworthy that previous studies have already pointed out limitations in FTIR analysis for detecting photooxidation processes in pigments contained in paints that are clearly visible to the naked eye [19,72].

While FTIR measurements may not indicate degradation of the additives, it is evident that the coatings undergo significant aesthetic changes that cannot be overlooked. Hence, in order to more precisely quantify the aesthetic deterioration of the different samples, gloss and color measurements were conducted while they were exposed in the UV-B chamber, as depicted in the graphs presented in Fig. 11. Fig. 11a illustrates the progression of gloss in the samples, depicting a notable decline during the initial hours of testing in sample REF and sample B. This decline is commonly linked to photooxidation processes and is particularly noticeable in samples with initially higher gloss values. In fact, this phenomenon is not apparent in sample BC, sample BCU samples, and the wooden panel, which exhibit high opacity from the outset. However, besides reflectance, what stands out most from the preceding Fig. 8 is the color alteration of the samples, depicted quantitatively in Fig. 11b. As anticipated, the wooden panel experiences substantial degradation, manifesting in a swift and pronounced shift in color. Likewise, the ΔE values of samples B and BC persistently rise throughout the test, indicating an ongoing deterioration of the pigment. Given the nearly identical behavior of the two samples, it can be inferred that the additional inclusion of the composite filler in sample BC does not influence the UV protection of the coating in any discernible manner. Remarkably, sample BCU exhibits superior performance compared to all others, displaying lower ΔE values even when compared to the REF sample. Additionally, a notable plateau is observed between 24 h and 48 h, while the curves of the other samples continue to ascend, indicating the effective protective function of the UV absorber incorporated into sample BCU.

Indeed, upon examining the trends depicted in the graphs of the three individual color coordinates L*, a*, and b*, it becomes apparent that sample BCU demonstrates remarkable stability, with minimal fluctuations. Conversely, both samples B and BC display decreases in a*, indicative of diminished redness, accompanied by noticeable increases in b*, signifying yellowing of the pigment.

Ultimately, the accelerated degradation test revealed the inadequate chromatic consistency of the bio-based pigment, leading to the loss of its characteristic red-burgundy color upon exposure to UV-B radiation. However, the experiments also showcased the excellent performance of the UV absorber, effectively minimizing the color fading of coating BCU. This outcome illustrates the feasibility of utilizing beetroot extracts as environmentally friendly pigments for paints, with their aesthetic longevity ensured through the incorporation of specialized UV absorber additives.

3.4. *Effect of the additive on the coating's barrier properties*

Having thus established the effectiveness of both the composite filler in enhancing the mechanical properties of the coating and the UV absorber in bolstering the color durability of the bio-based pigment, it is imperative to ensure that the incorporation of these additives does not compromise the barrier properties of the layer. After all, its primary role is to safeguard the wooden substrate.

Consequently, the samples underwent initial water absorption tests, the outcome of which is depicted in the graph presented in Fig. 12a, expressed as the water uptake by the coatings. Certainly, the wooden panel demonstrates markedly distinct behavior from the various coated samples, wherein the coating serves as a barrier agent. Initially, wood absorbs significant amounts of water during the initial hours of testing; subsequently, this absorption trend decelerates, suggesting a saturation of the surface layers of the wood. Conversely, the four coating series substantially diminish the solution uptake, yielding values that do not surpass 700 g/m^2 by the conclusion of the test. The consistent behavior observed across the four series of samples is particularly encouraging, indicating that the various additives do not facilitate water percolation within the acrylic matrix of the coating. This reaffirms previous assumptions regarding the reduced defectiveness observed in the three composite coatings. This aspect is vital but commonly disregarded: the inclusion of various fillers in acrylic paints has frequently diminished the paint's ability to act as a barrier, primarily because of the hydrophilic properties of the additive [94,95]. Nevertheless, the pigment displays significant sensitivity, attributed to its susceptibility to dissolve easily in water. Upon contact with the test solution, color loss occurs, leading to a noticeable aesthetic alteration in the coatings. This phenomenon is quantitatively illustrated by the graph in Fig. 12b, which clearly depicts a strong color change ΔE measured in the three coatings containing the beetroot pigment at the end of the test. This phenomenon is gradually mitigated in sample BC and sample BCU, primarily due to their initial lighter colors. Conversely, the gloss values (Fig. 12c) of the samples are not notably affected by contact with the test solution, except for sample REF, wherein its initially high reflectance experiences a considerable reduction.

These findings highlight concerns about potential consequences associated with exposing the coatings containing the pigment to liquid solutions, which could lead to discoloration. Consequently, to confirm this phenomenon, the samples underwent the cold liquid resistance test.

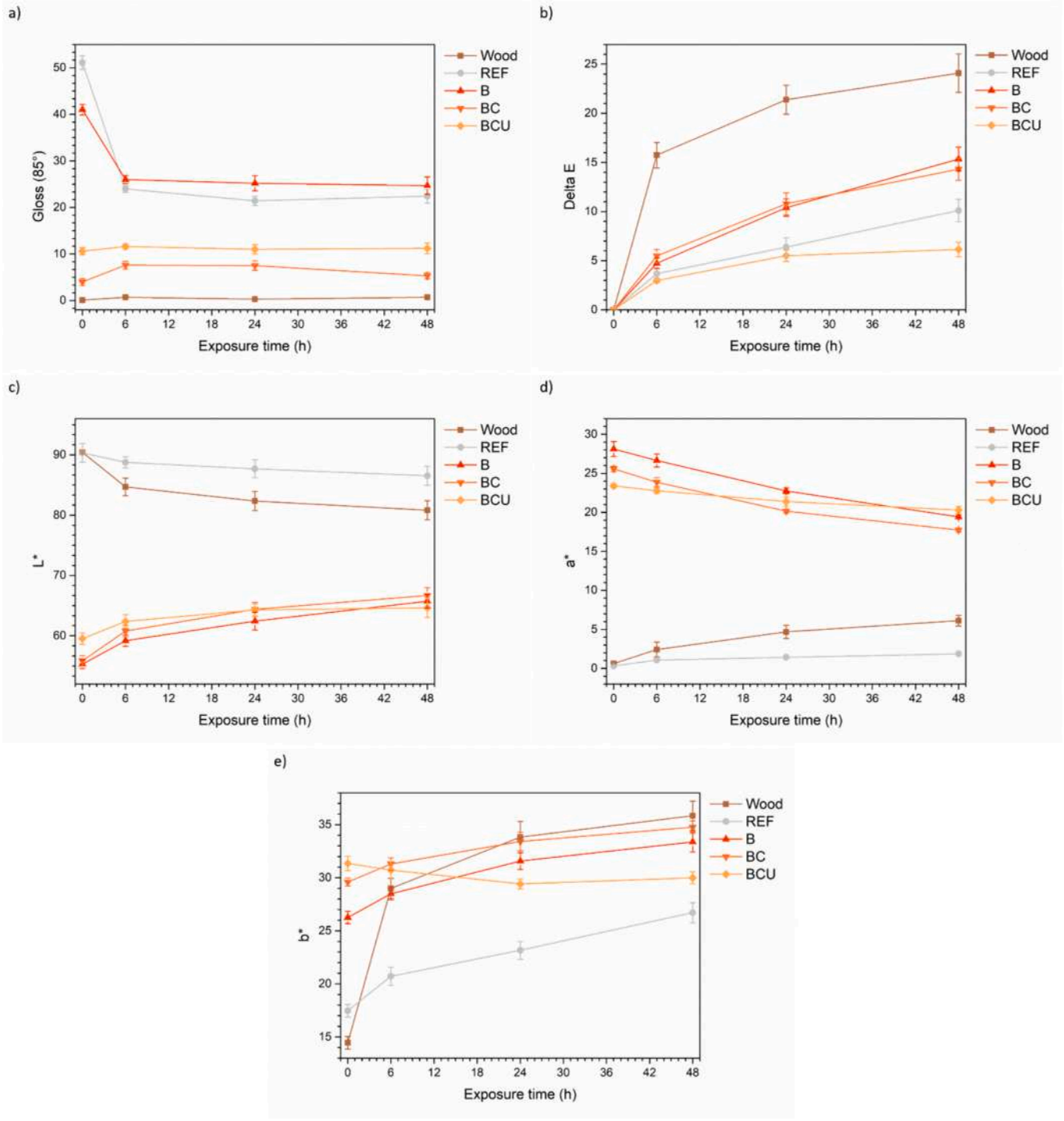

Fig. 11. Evolution of a) gloss, b) color change, c) L* coordinate, d) a* coordinate and e) b* coordinate, during the UV-B radiation exposure test.

Fig. 13a illustrates the test outcomes, showcasing the color change ΔE observed in the four sets of samples after coming into contact with the six chosen test liquids. Sample REF consistently demonstrates excellent performance, with very low ΔE values falling within the 0–1 range of the standard [96], indicative of minimal fading. Conversely, sample B reinforces and verifies the issues observed earlier, characterized by significant discoloration upon contact with aqueous solutions. Specifically, results obtained with NaCl solution, coffee, and acidic and basic solutions reveal color changes ΔE falling into categories 4–5 [96], signifying considerable alterations in color. On the other hand, acetone and oil, being non-aqueous solutions, do not impact the fading of the pigment, resulting in limited ΔE values for sample B. With the exception of the basic solution, which exhibits notable aggressiveness, the degree of fading appears relatively restrained in sample BC and in sample BCU. This can be attributed partly to their initially lighter color and also to the inert nature of both the reinforcing filler and the UV absorber upon contact with aqueous solutions, thereby mitigating the overall deterioration caused by the test liquids. Nonetheless, it is evident that both sample BC and sample BCU still undergo discernible aesthetic alterations, falling within color fading categories 3–4 [96]. Moreover, the different solutions induce varying degrees of change in gloss (Fig. 13b), resulting in either reductions or increases (as observed with olive oil) in

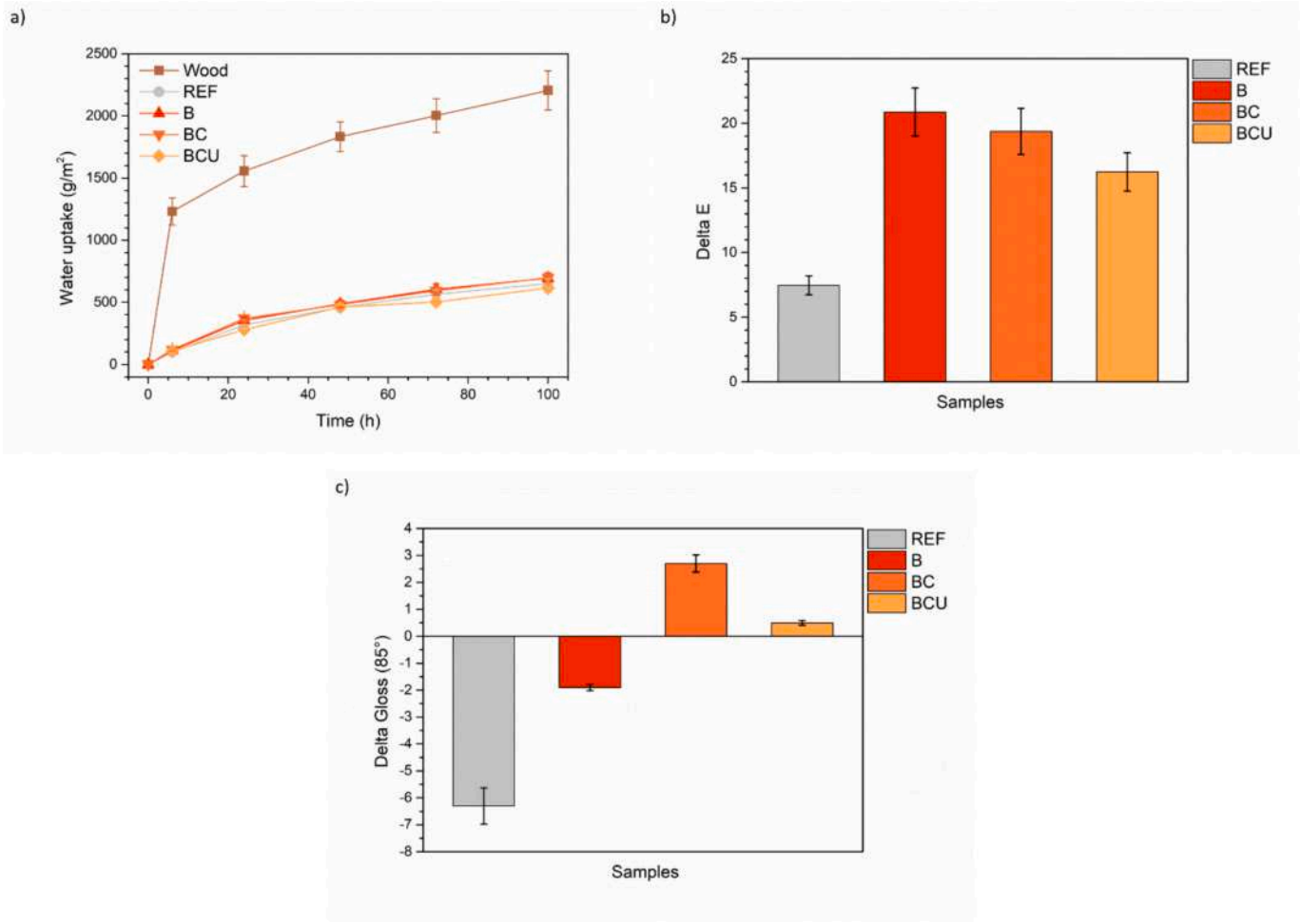

Fig. 12. a) monitoring the water absorption by the coatings during the test, resulting in subsequent final alterations in b) color change and c) gloss change.

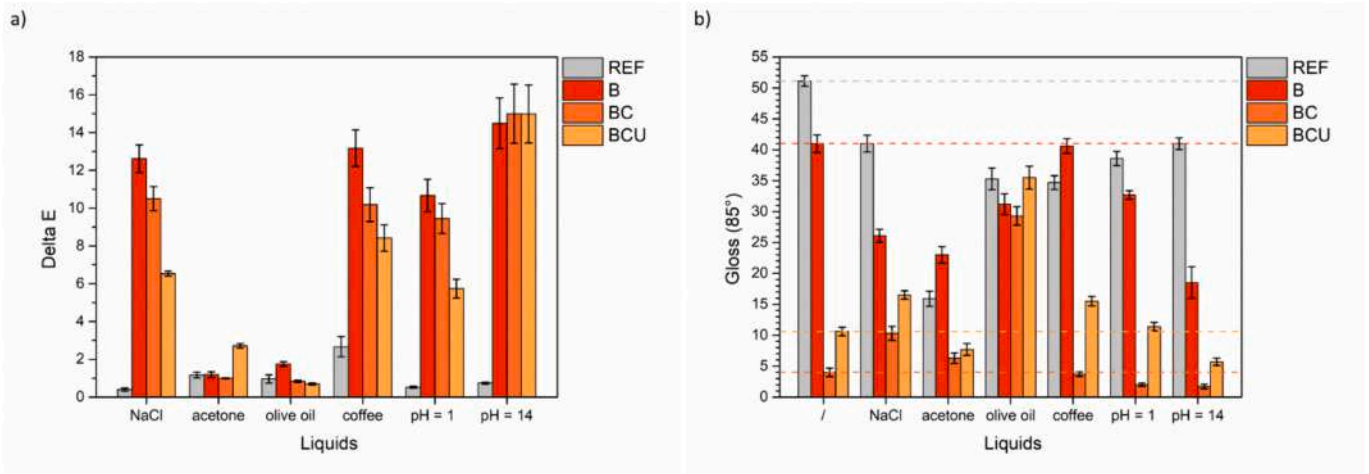

Fig. 13. Change in a) color and b) evolution of the gloss of the samples following the liquid resistance test.

the reflectance values of the coatings. Particularly, acetone notably diminishes the brightness of the samples, directly impacting the degradation of the acrylic matrix of the coating (see sample REF).

Hence, contact with diverse solutions yields consequences that are not always trivial in terms of aesthetics. Clearly, a crucial factor in this regard is closely linked to the barrier effect of the coating itself, which correlates with its level of hydrophobicity. Therefore, to assess the influence of the various additives in this regard, the samples underwent contact angle measurements. The images in Fig. 14 depict an example of a droplet created for a single series of samples. Additionally, the images display the average contact angle value, obtained from 10 measurements per sample. Over the first 60-s period after their deposition, the contact angle of the drops on all samples decreased by an average of about 2°, indicating slight absorption phenomena by the coatings. After

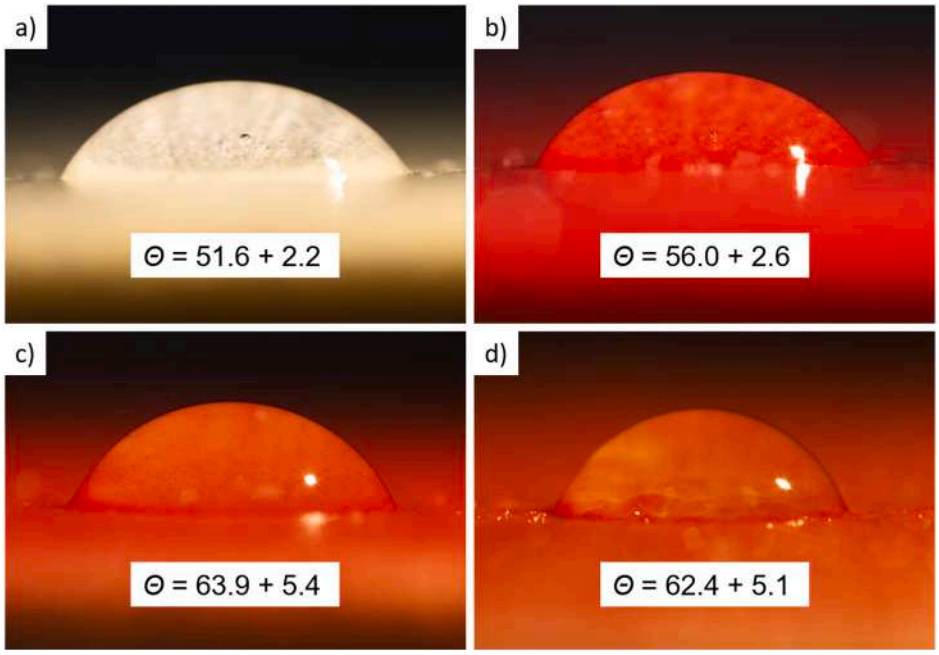

Fig. 14. Optical micrographs illustrating the contact angle measurements conducted with demineralized water for a) sample REF, b) sample B, c) sample BC, and d) sample BCU.

reaching 60 s, there was a stabilization in the evolution of the contact angles, revealing the true behavior of the samples. The results align with the findings of the roughness measurements: the contact angle increases proportionally with the surface roughness, as depicted in Fig. 3b. The diminished wettability observed in sample BC and in sample BCU is not attributed to specific hydrophobic characteristics of the composite filler or the UV absorber. Rather, numerous studies in the literature have underscored the correlation between surface roughness and the hydrophobicity of surfaces [97,98]. Ultimately, it can be concluded that the reinforcing filler does not compromise the barrier function of the coating; instead, it enhances its hydrophobic properties through a significant increase in surface roughness. However, it would be inaccurate to characterize sample BC and sample BCU as having hydrophobic surfaces, as their contact angle values remain relatively low [99]. Indeed, the earlier water uptake test demonstrated similar barrier behavior across the four series of samples.

Therefore, ultimately, the additives do not appear to compromise the barrier properties of the coating. However, in some instances, they do decrease its wettability, owing to significant alterations in surface texture. Nevertheless, the issue persists regarding the high susceptibility of the beetroot pigment's color to fading upon contact with aqueous solutions. This aspect does not recommend its usage in paints that might encounter high humidity environments.

4. Conclusions

This research investigates the combined impact of a bio-based pigment extracted from red beetroot, a composite reinforcing filler, and a UV absorber when used as additives in wood paints. SEM analyses have revealed that the additives do not introduce flaws in the coating but they substantially alter both its color and gloss. Indeed, the pigment induces a color change of approximately 45 units, whereas the multifunctional filler leads to a threefold increase in surface roughness. Thus, the synergy among the three additives must be deliberately tailored based on the desired aesthetic outcome for the coating.

On the other hand, while the functional filler added to the paint to enhance its mechanical properties does not notably elevate the coating's hardness, it does significantly enhance its resistance to abrasion. This is evidenced by a reduction of approximately 29 % in the mass removed due to the Taber test after 3000 cycles. This phenomenon is linked to the low friction coefficient of the PTFE component within the composite filler, which effectively diminishes material removal processes under shear stress.

The UV absorber fulfills its intended role, which is to enhance the color consistency of the bio-based pigment when exposed to solar radiation. Specifically, the BCU sample demonstrates a decreased E color change after 48 h of exposure in a UV-B chamber, dropping from approximately 15 units in sample B to only 5.

In conclusion, the diverse liquid resistance tests have demonstrated that the three additives do not adversely affect the barrier properties of the coating. Nevertheless, the composite filler leads to a minor reduction in wettability due to notable changes in the surface texture of the coating. Nonetheless, the notable propensity of the pigment to fade upon contact with aqueous solutions poses a significant concern, particularly in the application of this specific bio-based additive in outdoor paint formulations.

Ultimately, the array of tests conducted has showcased how each of the three additives fulfills a distinct function, and their combined utilization in sample BCU yields multiple advantages. These include vibrant color retention even after exposure to UV radiation and enhanced mechanical durability of the coating. Thus, the study underscores the critical challenges associated with using natural pigments, which often face issues with chromatic consistency due to external factors like light, oxygen, and temperature. However, this research proposes a potential solution to these challenges by employing UV absorbers, which have been extensively studied and refined at an industrial level. These UV absorbers can enhance the chromatic durability of the pigment without compromising the protective properties of the coating. Additionally, the strategic use of an innovative composite filler enhances the mechanical properties of the coating without compromising its aesthetics, demonstrating good compatibility with the bio-based pigment. However, future research should focus on exploring more environmentally-friendly alternatives to additives containing PTFE.

CRediT authorship contribution statement

Massimo Calovi: Writing – original draft, Validation, Methodology, Investigation, Data curation, Conceptualization. **Stefano Rossi:** Writing – review & editing, Supervision, Resources, Project administration.

Declaration of competing interest

The authors declare that they have no known competing financial interests or personal relationships that could have appeared to influence the work reported in this paper.

Data availability

Data will be made available on request.

Acknowledgments

The authors greatly acknowledge the contributions of Stefano Di Blase (ICA Group, Civitanova Marche, MC, Italy) for the paint supply. Moreover, special thanks should be given to Alberto Pinzo (Garzanti Specialties, Milan, Italy) and Massimo Villano (3V Sigma, Bergamo, Italy) regarding the beetroot powder and UV absorber supply, respectively. Finally, the important contribution of Gianluca Cometti (Azelis Italia, Milan, Italy) and Donna Gilbert (Micro Powders, Tarrytown, NY, USA) must be recognized, for the supply of composite filler. The publication was created with the co-financing of the European Union – FSE-REACT-EU, PON Research and Innovation 2014-2020 DM1062/2021.

Funding

This research did not receive any specific grant from funding agencies in the public, commercial, or not-for-profit sectors.

Appendix A. Supplementary data

Supplementary data to this article can be found online at https://doi.org/10.1016/j.porgcoat.2024.108529.

References

[1] J.K. Kim, K. Pal, Recent Advances in the Processing of Wood-plastic Composites, Springer-Verlag, Berlin Heidelberg, 2010.
[2] R.B. Hoadley, Chemical and Physical Properties of Wood, the Structural Conservation of Panel Paintings: Proceedings. Part 1: Wood Science and Technology, 1998, pp. 2–20.
[3] J. Hao, X. Wu, G. Oporto, W. Liu, J. Wang, Structural analysis and strength-to-weight optimization of wood-based sandwich composite with honeycomb core under three-point flexural test, Eur. J. Wood Wood Prod. 78 (2020) 1195–1207.
[4] M. Pánek, L. Reinprecht, Colour stability and surface defects of naturally aged wood treated with transparent paints for exterior constructions, Wood Res. 59 (2014) 421–430.
[5] F. Zareanshahraki, V. Mannari, Formulation and optimization of radiation-curable nonisocyanate polyurethane wood coatings by mixture experimental design, J. Coat. Technol. Res. 18 (2021) 695–715.
[6] R. Bansal, S. Nair, K.K. Pandey, UV resistant wood coating based on zinc oxide and cerium oxide dispersed linseed oil nano-emulsion, Mater. Today Commun. 30 (2022) 103177.
[7] V. Jirouš-Rajković, J. Miklečić, Enhancing weathering resistance of wood—a review, Polymers 13 (2021) 1980.
[8] S. Veigel, G. Grüll, S. Pinkl, M. Obersriebnig, U. Müller, W. Gindl-Altmutter, Improving the mechanical resistance of waterborne wood coatings by adding cellulose nanofibres, React. Funct. Polym. 85 (2014) 214–220.
[9] P. Hochmańska-Kaniewska, D. Janiszewska, T. Oleszek, Enhancement of the properties of acrylic wood coatings with the use of biopolymers, Prog. Org. Coat. 162 (2022) 106522.
[10] S.M. Miri Tari, A. Tarmian, M. Azadfallah, Improving fungal decay resistance of solvent and waterborne polyurethane-coated wood by free and microencapsulated thyme essential oil, J. Coat. Technol. Res. 19 (2022) 959–966.
[11] G. Janin, J.C. Gonçalez, R.A. Ananías, B. Charrier, G.F.d. Silva, A. Dilem, Aesthetics appreciation of wood colour and patterns by colorimetry, in: Part 1. Colorimetry Theory for the CIELab System, 2001.
[12] M.C. Wiemann, Characteristics and availability of commercially important woods, Forest Products Laboratory. Wood handbook: wood as an engineering material, in: Madison: United States Department of Agriculture: Forest Service, 2010.
[13] X. Yan, Y. Chang, X. Qian, Effect of the concentration of pigment slurry on the film performances of waterborne wood coatings, Coatings 9 (2019) 635.
[14] M. Calovi, A. Zanardi, S. Rossi, Recent advances in bio-based wood protective systems: a comprehensive review, Appl. Sci. 14 (2024) 736.
[15] Y. Liu, Z. Yu, Y. Zhang, H. Wang, Microbial dyeing for inoculation and pigment used in wood processing: opportunities and challenges, Dyes Pigments 186 (2021) 109021.
[16] S.M. Vega Gutierrez, D.W. Stone, R. He, P.T. Vega Gutierrez, Z.M. Walsh, S. C. Robinson, Potential use of the pigments from Scytalidium cuboideum and Chlorociboria aeruginosa to prevent 'Greying' Decking and other outdoor wood products, Coatings 11 (2021) 511.
[17] Y. Liu, Y. Zhang, Z. Yu, C. Qi, R. Tang, B. Zhao, H. Wang, Y. Han, Microbial dyes: dyeing of poplar veneer with melanin secreted by Lasiodiplodia theobromae isolated from wood, Appl. Microbiol. Biotechnol. 104 (2020) 3367–3377.
[18] M. Calovi, S. Rossi, From wood waste to wood protection: new application of black bio renewable water-based dispersions as pigment for bio-based wood paint, Prog. Org. Coat. 180 (2023) 107577.
[19] M. Calovi, S. Rossi, Eco-friendly multilayer coating harnessing the functional features of Curcuma-based pigment and Rice bran wax as a hydrophobic filler, Materials 16 (2023) 7086.
[20] M. Calovi, S. Rossi, Comparative analysis of the advantages and disadvantages of utilizing spirulina-derived pigment as a bio-based colorant for wood impregnator, Coatings 13 (2023) 1154.
[21] K. Prathiksha, S.J.E. Priyadharshini, J. Jacob, A.V. Jayakumar, P.H. Rao, Microalgal pigments as natural hues in environmentally-sustainable and commercially-prospective biopaints, J. Appl. Phycol. (2023) 1–14.
[22] M. Calovi, S. Rossi, Synergistic contribution of bio-based additives in wood paint: the combined effect of pigment deriving from spirulina and multifunctional filler based on carnauba wax, Prog. Org. Coat. 182 (2023) 107713.
[23] M. Calovi, S. Rossi, Impact of high concentrations of cellulose fibers on the morphology, durability and protective properties of wood paint, Coatings 13 (2023) 721.
[24] M. Calovi, S. Rossi, Exploring polyamide 11 as a novel renewable resource-based filler in wood paint: investigating aesthetic aspects and durability impact of the composite coating, Prog. Org. Coat. 188 (2024) 108262.
[25] M. Calovi, S. Rossi, The impact of stainless steel flakes as a novel multifunctional pigment for wood coatings, J. Coat. Technol. Res. (2024).
[26] C.M. Pacheco, B.A. Cecilia, G. Reyes, C. Oviedo, A. Fernández-Pérez, M. Elso, O. J. Rojas, Nanocomposite additive of SiO_2/TiO_2/nanocellulose on waterborne coating formulations for mechanical and aesthetic properties stability on wood, Mater. Today Commun. 29 (2021) 102990.
[27] J. Jusic, S. Tamantini, M. Romagnoli, V. Vinciguerra, E. Di Mattia, F. Zikeli, M. Cavalera, G. Scarascia Mugnozza, Improving sustainability in wood coating: testing lignin and cellulose nanocrystals as additives to commercial acrylic wood coatings for bio-building, iForest-Biogeosci. For. 14 (2021) 499.
[28] H. Řezbová, A. Belová, O. Škubna, Sugar beet production in the European Union and their future trends, in: Agris on-line Papers in Economics and Informatics 5, 2013, pp. 165–178.
[29] P. Mirmiran, Z. Houshialsadat, Z. Gaeini, Z. Bahadoran, F. Azizi, Functional properties of beetroot (Beta vulgaris) in management of cardio-metabolic diseases, Nutr. Metab. 17 (2020) 1–15.
[30] A.M. Salamatullah, K. Hayat, M.S. Alkaltham, M.A. Ahmed, S. Arzoo, F.M. Husain, A.M. Al-Dossari, G. Shamlan, L.N. Al-Harbi, Bioactive and antimicrobial properties of oven-dried beetroot (pulp and peel) using different solvents, Processes 9 (2021) 588.
[31] T. Nahla, S. Wisam, N. Tariq, Antioxidant activities of beetroot (Beta vulgaris L.) extracts, Pak. J. Nutr. 17 (2018) 500–505.
[32] S. Kumar, M.S.-L. Brooks, Use of red beet (Beta vulgaris L.) for antimicrobial applications—a critical review, Food Bioprocess Technol. 11 (2018) 17–42.
[33] V. Prieto-Santiago, M.M. Cavia, S.R. Alonso-Torre, C. Carrillo, Relationship between color and betalain content in different thermally treated beetroot products, J. Food Sci. Technol. 57 (2020) 3305–3313.
[34] Y. Fu, J. Shi, S.-Y. Xie, T.-Y. Zhang, O.P. Soladoye, R.E. Aluko, Red beetroot betalains: perspectives on extraction, processing, and potential health benefits, J. Agric. Food Chem. 68 (2020) 11595–11611.
[35] K. Ravichandran, N.M.M.T. Saw, A.A. Mohdaly, A.M. Gabr, A. Kastell, H. Riedel, Z. Cai, D. Knorr, I. Smetanska, Impact of processing of red beet on betalain content and antioxidant activity, Food Res. Int. 50 (2013) 670–675.
[36] M. Noraini, The characterization of beetroot pigment as surface coating, Int. J. Adv. Trends Comput. Sci. Eng. 8 (2019) 121–125.
[37] M. Yeniocak, O. Goktas, M. Colak, E. Ozen, M. Ugurlu, Natural coloration of wood material by red beetroot (Beta vulgaris) and determination color stability under UV exposure, Maderas. Ciencia y tecnología 17 (2015) 711–722.
[38] P. Šimon, M. Fratričová, P. Schwarzer, H.-W. Wilde, Evaluation of the residual stability of polyurethane automotive coatings by DSC: equivalence of Xenotest and desert weathering tests and the synergism of stabilizers, J. Therm. Anal. Calorim. 84 (2006) 679–692.
[39] C. Queant, V. Landry, P. Blanchet, D. Schorr, Synthesis and incorporation of poly (methyl methacrylate) microspheres with UV stabilizers in wood clear coating binder, J. Coat. Technol. Res. 14 (2017) 1411–1422.
[40] S. Nikafshar, O. Zabihi, M. Ahmadi, A. Mirmohseni, M. Taseidifar, M. Naebe, The effects of UV light on the chemical and mechanical properties of a transparent

epoxy-diamine system in the presence of an organic UV absorber, Materials 10 (2017) 180.
[41] Y. Liu, Y. Liu, J. Lin, H. Tan, C. Zhang, UV-protective treatment for Vectran® fibers with hybrid coatings of TiO2/organic UV absorbers, J. Adhes. Sci. Technol. 28 (2014) 1773–1782.
[42] M. Shenoy, Y. Marathe, Studies on synergistic effect of UV absorbers and hindered amine light stabilisers, Pigm. Resin Technol. 36 (2007) 83–89.
[43] F. Aloui, A. Ahajji, Y. Irmouli, B. George, B. Charrier, A. Merlin, Inorganic UV absorbers for the photostabilisation of wood-clearcoating systems: comparison with organic UV absorbers, Appl. Surf. Sci. 253 (2007) 3737–3745.
[44] J.J. Balatinecz, D.E. Kretschmann, A. Leclercq, Achievements in the utilization of poplar wood–guideposts for the future, For. Chron. 77 (2001) 265–269.
[45] J.J. Balatinecz, D.E. Kretschmann, Properties and utilization of poplar wood, in: Poplar Culture in North America, 2001, pp. 277–291.
[46] ASTM D523-14 - Standard Test Method for Specular Gloss, West Conshohocken, ASTM International, PA, 2014, pp. 1–12.
[47] ISO 2815-2000, Determinazione della durezza con il metodo di penetrazione Buchholz, UNI - Ente Nazionale Italiano di Unificazione, 2000, pp. 1–10.
[48] ASTM D4060, Standard Test Method for Abrasion Resistance of Organic Coatings by the Taber Abraser, West Conshohocken (PA): ASTM International, 2010, pp. 1–13.
[49] ASTM D4587-11(2019)e1, Standard Practice for Fluorescent UV-Condensation Exposures of Paint and Related Coatings, West Conshohocken (PA): ASTM International, 2019, pp. 1–6.
[50] EN927-05, Paints and varnishes - coating materials and coating systems for exterior wood - part 5: assessment of the liquid water permeability, in: European Standard, 2005, pp. 1–18.
[51] UNI EN 12720-14, Assessment of surface resistance to cold liquids, in: European Committee for Standardization, 2014, pp. 1–4.
[52] ASTM D7334–08, Standard practice for surface wettability of coatings, substrates and pigments by advancing contact angle measurement, in: West Conshohocken (PA): ASTM International, 2008, pp. 1–3.
[53] ASTM-E308-18, Standard Practice for Computing the Colors of Objectives by Using the CIE System, West Conshohocken, ASTM International, PA, 2018, pp. 1–45.
[54] W. Mokrzycki, M. Tatol, Colour difference ΔE - a survey, Mach. Graph. Vis. 20 (2011) 383–411.
[55] H. Yari, S. Moradian, B. Ramazanzade, A. Kashani, N. Tahmasebi, The effect of basecoat pigmentation on mechanical properties of an automotive basecoat/clearcoat system during weathering, Polym. Degrad. Stab. 94 (2009) 1281–1289.
[56] B.V. Gregorovich, K. Adamsons, L. Lin, Scratch and mar and other mechanical properties as a function of chemical structure for automotive refinish coatings, Prog. Org. Coat. 43 (2001) 175–187.
[57] M. Calovi, S. Rossi, Evaluating the versatility of stainless steel flakes and magnetite powder as polyvalent additives for wood paints, J. Mater. Res. Technol. 29 (2024) 1010–1024.
[58] A. Kaboorani, N. Auclair, B. Riedl, V. Landry, Mechanical properties of UV-cured cellulose nanocrystal (CNC) nanocomposite coating for wood furniture, Prog. Org. Coat. 104 (2017) 91–96.
[59] A. Momber, M. Irmer, T. Marquardt, Effects of polymer hardness on the abrasive wear resistance of thick organic offshore coatings, Prog. Org. Coat. 146 (2020) 105720.
[60] A. Momber, M. Irmer, Taber abrasive wear resistance of organic offshore wind power coatings at varying normal forces, J. Coat. Technol. Res. 18 (2021) 729–740.
[61] D. Gu, L. Zhang, S. Chen, K. Song, S. Liu, Significant reduction of the friction and wear of PMMA based composite by filling with PTFE, Polymers 10 (2018) 966.
[62] K.R. Makinson, D. Tabor, The friction and transfer of polytetrafluoroethylene, Proc. Roy. Soc. Lond. Ser. A Math. Phys. Sci. 281 (1964) 49–61.
[63] S. Biswas, K. Vijayan, Friction and wear of PTFE—a review, Wear 158 (1992) 193–211.
[64] E. Dhanumalayan, G.M. Joshi, Performance properties and applications of polytetrafluoroethylene (PTFE)—a review, Adv. Compos. Hybrid Mater. 1 (2018) 247–268.
[65] M. Sajid, M. Ilyas, PTFE-coated non-stick cookware and toxicity concerns: a perspective, Environ. Sci. Pollut. Res. 24 (2017) 23436–23440.
[66] M. Beekman, P. Zweers, A. Muller, W. De Vries, P. Janssen, M. Zeilmaker, Evaluation of substances used in the GenX technology by Chemours, Dordrecht, RIVM Lett. Rep. 2016-0174 (2016).
[67] Z. Wang, I.T. Cousins, M. Scheringer, K. Hungerbühler, Fluorinated alternatives to long-chain perfluoroalkyl carboxylic acids (PFCAs), perfluoroalkane sulfonic acids (PFSAs) and their potential precursors, Environ. Int. 60 (2013) 242–248.
[68] https://www.micropowders.com/polytuf-1229.html (accessed on 29-04-2024).
[69] I. Groeneveld, M. Kanelli, F. Ariese, M.R. van Bommel, Parameters that affect the photodegradation of dyes and pigments in solution and on substrate–an overview, Dyes Pigments 210 (2023) 110999.
[70] U. Bali, E. Çatalkaya, F. Şengül, Photodegradation of Reactive Black 5, Direct Red 28 and Direct Yellow 12 using UV, UV/H2O2 and UV/H2O2/Fe2+: a comparative study, J. Hazard. Mater. 114 (2004) 159–166.
[71] R. Arshad, T. Bokhari, T. Javed, I. Bhatti, S. Rasheed, M. Iqbal, A. Nazir, S. Naz, M. Khan, M. Khosa, Degradation product distribution of Reactive Red-147 dye treated by UV/H2O2/TiO2 advanced oxidation process, J. Mater. Res. Technol. 9 (2020) 3168–3178.
[72] M. Calovi, V. Coroneo, S. Palanti, S. Rossi, Colloidal silver as innovative multifunctional pigment: the effect of Ag concentration on the durability and biocidal activity of wood paints, Prog. Org. Coat. 175 (2023) 107354.
[73] E. Attoe, J. Von Elbe, Photochemial degradation of betanine and selected anthocyanins, J. Food Sci. 46 (1981) 1934–1937.
[74] K.M. Herbach, F.C. Stintzing, R. Carle, Betalain stability and degradation—structural and chromatic aspects, J. Food Sci. 71 (2006) R41–R50.
[75] R. Castellar, J.M. Obón, M. Alacid, J.A. Fernández-López, Color properties and stability of betacyanins from Opuntia fruits, J. Agric. Food Chem. 51 (2003) 2772–2776.
[76] F. Delgado-Vargas, A. Jiménez, O. Paredes-López, Natural pigments: carotenoids, anthocyanins, and betalains—characteristics, biosynthesis, processing, and stability, Crit. Rev. Food Sci. Nutr. 40 (2000) 173–289.
[77] H.M. Azeredo, Betalains: properties, sources, applications, and stability–a review, Int. J. Food Sci. Technol. 44 (2009) 2365–2376.
[78] P. Esquivel, Handbook on Natural Pigments in Food and Beverages, in, Academic Press, Cambridge, 2016.
[79] A. Huang, J. Von Elbe, Stability comparison of two betacyanine pigments—amaranthine and betanine, J. Food Sci. 51 (1986) 670–674.
[80] A. Martínez-Romo, R. González-Mota, J. Soto-Bernal, I. Rosales-Candelas, Investigating the degradability of HDPE, LDPE, PE-Bio, and pe-oxo films under UV-B radiation, J. Spectrosc. 2015 (2015).
[81] B.K. Tsai, C.C. Cooksey, D.W. Allen, C.C. White, E. Byrd, D. Jacobs, Exposure study on UV-induced degradation of PTFE and ceramic optical diffusers, Appl. Opt. 58 (2019) 1215–1222.
[82] S.N.A. Kumar, S.K. Ritesh, G. Sharmila, C. Muthukumaran, Extraction optimization and characterization of water soluble red purple pigment from floral bracts of Bougainvillea glabra, Arab. J. Chem. 10 (2017) S2145–S2150.
[83] G.A. Molina, A.R. Hernández-Martínez, M. Cortez-Valadez, F. García-Hernández, M. Estevez, Effects of tetraethyl orthosilicate (TEOS) on the light and temperature stability of a pigment from Beta vulgaris and its potential food industry applications, Molecules 19 (2014) 17985–18002.
[84] V. Rotich, P. Wangila, J. Cherutoi, FT-IR analysis of Beta vulgaris peels and pomace dye extracts and surface analysis of optimally dyed-Mordanted cellulosic fabrics, J. Chemother. 2022 (2022).
[85] Y. Cai, M. Sun, H. Wu, R. Huang, H. Corke, Characterization and quantification of betacyanin pigments from diverse Amaranthus species, J. Agric. Food Chem. 46 (1998) 2063–2070.
[86] D. Sengupta, B. Mondal, K. Mukherjee, Visible light absorption and photo-sensitizing properties of spinach leaves and beetroot extracted natural dyes, Spectrochim. Acta A Mol. Biomol. Spectrosc. 148 (2015) 85–92.
[87] L. Aztatzi-Rugerio, S.Y. Granados-Balbuena, Y. Zainos-Cuapio, E. Ocaranza-Sánchez, M. Rojas-López, Analysis of the degradation of betanin obtained from beetroot using Fourier transform infrared spectroscopy, J. Food Sci. Technol. 56 (2019) 3677–3686.
[88] S.N. Monteiro, F.M. Margem, R.L. Loiola, F.S. de Assis, M.P. Oliveira, Characterization of Banana Fibers Functional Groups by Infrared Spectroscopy, Materials Science Forum, Trans Tech Publ, in, 2014, pp. 250–254.
[89] J. Gulmine, P. Janissek, H. Heise, L. Akcelrud, Polyethylene characterization by FTIR, Polym. Test. 21 (2002) 557–563.
[90] J. Piwowarczyk, R. Jędrzejewski, D. Moszyński, K. Kwiatkowski, A. Niemczyk, J. Baranowska, XPS and FTIR studies of polytetrafluoroethylene thin films obtained by physical methods, Polymers 11 (2019) 1629.
[91] S. Wang, J. Li, J. Suo, T. Luo, Surface modification of porous poly (tetrafluoraethylene) film by a simple chemical oxidation treatment, Appl. Surf. Sci. 256 (2010) 2293–2298.
[92] R.A. Robayo-Salazar, R.M. de Gutiérrez, F. Puertas, Effect of metakaolin on natural volcanic pozzolan-based geopolymer cement, Appl. Clay Sci. 132 (2016) 491–497.
[93] C. Finocchiaro, G. Barone, P. Mazzoleni, C. Leonelli, A. Gharzouni, S. Rossignol, FT-IR study of early stages of alkali activated materials based on pyroclastic deposits (Mt. Etna, Sicily, Italy) using two different alkaline solutions, Constr. Build. Mater. 262 (2020) 120095.
[94] M. Kluge, S. Veigel, S. Pinkl, U. Henniges, C. Zollfrank, A. Rössler, W. Gindl-Altmutter, Nanocellulosic fillers for waterborne wood coatings: reinforcement effect on free-standing coating films, Wood Sci. Technol. 51 (2017) 601–613.
[95] M. Calovi, S. Rossi, Functional olive pit powders: the role of the bio-based filler in reducing the water uptake phenomena of the waterborne paint, Coatings 13 (2023) 442.
[96] GB/T11186.3-90, Method of Measurement of Coating Color. Part III: Calculation of Chromatic Aberration, Standardization Administration of the People's Republic of China: Beijing, 1990, pp. 1–12.
[97] X. Wang, Z. Qu, G. Ren, Collective enhancement in hydrophobicity and electrical conductivity of gas diffusion layer and the electrochemical performance of PEMFCs, J. Power Sources 575 (2023) 233077.
[98] X. Wang, Z. Qu, T. Lai, G. Ren, W. Wang, Enhancing water transport performance of gas diffusion layers through coupling manipulation of pore structure and hydrophobicity, J. Power Sources 525 (2022) 231121.
[99] K.-Y. Law, Definitions for hydrophilicity, hydrophobicity, and superhydrophobicity: getting the basics right, in, ACS Publ. (2014) 686–688.